HELSINKI UNIVERSITY OF TECHNOLOGY
Faculty of Electronics, Communications and Automation

Antti Lankila

Simulation Model for an Active Noise Control System - Development and Validation

Master's Thesis submitted in partial fulfillment of the requirements for the degree of Master of Science in Technology.

Espoo, February 18, 2008

Supervisor: Professor Vesa Välimäki
Instructor: Lic.Tech. Marko Antila

HELSINKI UNIVERSITY OF TECHNOLOGY

ABSTRACT OF THE MASTER'S THESIS

Author:	Antti Lankila
Name of the thesis:	Simulation Model for an Active Noise Control System – Development and Validation
Date:	18 Feb 2008 **Number of pages**: 7+60
Programme:	Communications Engineering
Supervisor:	Professor Vesa Välimäki
Instructor:	Lic. Tech. Marko Antila

Nowadays computers are able to simulate active noise control systems, so it is possible to save costs and research the systems more deeply with simulation models. The development of an ANC simulation model can be divided into two parts: the modelling of primary noise and the modelling of secondary, or counter, noise. The noise made by the ANC system can be modelled only if we have the information of primary noise. For successful simulation of secondary noise, we have to model the control system and its interaction with the surrounding acoustical space.

In ANC applications, sensors can seldom be placed near the listeners ears. In that sense, it is valuable to inspect the effect of transducer locations on the total noise at the listener's ears.

In this thesis, a simulation model for an ANC system with a one-channel tonal feedforward control system is developed and verified through comparative simulations and measurements in separate observation points. The noise excitation used in the verification phase is tonal and it has dynamic frequency content. The simulation model has been developed in MATLAB Simulink environment. The control system has been coded in a digital signal processor.

Keywords: Active Noise Control, simulation model, modelling, control system.

TEKNILLINEN KORKEAKOULU DIPLOMITYÖN TIIVISTELMÄ

Tekijä:	Antti Lankila
Työn nimi:	Aktiivisen äänenhallintajärjestelmän simulaatiomallin kehittäminen ja validointi
Päivämäärä:	18. helmikuuta 2008 **Sivuja**: 7+60
Koulutusohjelma:	Tietoliikennetekniikka
Työn valvoja:	Professori Vesa Välimäki
Työn ohjaaja:	TkL Marko Antila

Aktiivisen äänenhallintajärjestelmän suunnittelu ja toteutus vaatii akustiikan, mekaniikan ja elektroniikan osaamista. Nykyiset tietokoneet mahdollistavat aktiivisten äänenhallintajärjestelmien simuloinnin, joten on mahdollista sekä säästää suunnittelutyön resursseja että tutkia syvällisemmin järjestelmän riippuvuuksia simulaatiomallien avulla.

Järkevin tapa toteuttaa simulaatiomalli riippuu käyttötarkoituksesta ja lähtökohdista. Simulaatiomallin kehittäminen jakautuu kahteen osaan – melun ja vastaäänen mallintamiseen. Melu on mallinnettava, mikäli vaimennettavaa ympäristöä herätteineen ei ole olemassa. Äänenhallintajärjestelmän tuottamaan vastaääntä ei voida simuloida ilman tarkkaa tietoa melusta. Vastaäänen mallintamisessa on mallinnettava säätöjärjestelmä ja sen vuorovaikutus akustisen ympäristön kanssa.

Aktiivisen äänenhallinnan sovelluksissa anturit voidaan harvoin sijoittaa kuulijan korvien välittömään läheisyyteen. Tästä syystä on usein hyödyllistä tutkia sitä, miten erilaiset anturi- ja kaiutinpaikat vaikuttavat korvalla kuultavaan ääneen.

Tässä diplomityössä mallinnetaan olemassa oleva yksikanavainen myötäkytketty äänenhallintajärjestelmä ja tutkitaan simulaatiomallin ja mittauksen vastaavuutta muuttuvalla meluherätteellä eri tarkkailupisteissä. Simulaatiomalli kehitetään MATLAB Simulink ympäristöön. Säätöjärjestelmänä käytetään digitaalista signaaliprosessoria.

Avainsanat: Aktiivinen äänenhallinta, simulaatiomalli, mallinnus, säätöjärjestelmä.

Acknowledgements

I would like to thank Team Leader Hannu Nykänen and Technology Manager Pekka Koskinen for giving me this opportunity to make my thesis at VTT. I would also like to thank Research Scientist Marko Antila for being my thesis instructor. A word of thanks belongs to the acoustically oriented group of scientist here in Tampere for the friendly atmosphere. I would especially like to thank Research Scientist Velipekka Mellin for many inspiring and clarifying conversations and helping me in my work here at VTT.

Finally, I would like to thank you, Maria, for your support and endless love.

Tampere, 18th of February 2008

Antti Lankila

Contents

List of Abbreviations

AD	Analogue-to-Digital
ANC	Active Noise Control
DA	Digital-to-Analogue
DFT	Discrete Fourier Transform
DSK	(Texas Instruments') Digital signal processing Starter Kit
DSP	Digital Signal Processor
FXLMS	Filtered-x Least Mean Square
LMS	Least Mean Square
MLS	Maximum-Length Sequence
MSE	Mean Square Error

List of Symbols

$*$	Convolution operator
∇	Gradient operator
$\frac{\partial}{\partial w(n)}$	Gradient of the mean square error surface
$\gamma^2(f)$	Coherence function
μ	Convergence factor in LMS algorithm
$\xi(n)$	Mean square error
$c(n)$	Command signal in Command-FXLMS algorithm
$d(n)$	Desired signal
$E[\cdot]$	Expectation value operator
$e(n)$	Error signal
$e'(n)$	Pseudoerror signal in Command-FXLMS algorithm
$e_p(n)$	Error signal in physical sensor location
$\hat{e}_v(n)$	Estimate of the virtual error signal
$F[\cdot]$	Fourier transform operator
$F^{-1}[\cdot]$	Inverse Fourier transform operator

$H_e(\omega)$	Fourier transform of the impulse response of the secondary path
h_e	Impulse response of the secondary path
$\lg(\cdot)$	Common logarithm
$NR(f)$	Noise Reduction function
p_p	Primary or noise sound pressure
$\hat{p}_p(n)$	Estimate of primary sound pressure
$\hat{p}_{ps}(n)$	Estimate of secondary noise component in physical sensor location
p_s	Secondary or anti-noise sound pressure
p_{tot}	Total sound pressure, sum of primary and secondary sound pressures
p_v	Virtual sound pressure
$\hat{p}_{vs}(n)$	Estimate of secondary sound pressure in location of virtual sensor
$S(z)$	Transfer function of the secondary path
$U(z)$	Transfer function of the unknown path
$w_l(n)$	Adaptive filter coefficient
$x(n)$	Reference signal
$x'(n)$	Filtered reference signal in FXLMS
$y(t)$	Secondary source input or control system output signal

1 Introduction

Active noise control is still awaiting a major breakthrough. The general increase in well-being and the desire for luxury will some day meet the decreasing price of practical active noise control systems in many areas. In some applications, like in active headsets, the breakthrough has already happened. The price of headsets with an active noise control feature is not much higher than the price of traditional headsets, meaning the decision to make an additional investment in a better listening experience is easily made. In some other potential application areas, like in the automotive industry, the challenges for active noise control are greater and there are not many practical applications of ANC. The broad interest in lightweight structures will surely generate noise-related challenges and make active noise control more attractive in the automotive industry as well.

Although the principles of acoustics and the basic algorithms for active noise control were invented quite a while ago, there is still a long way from theory to reality. In general, active noise control applications are still quite expensive and challenging to design. All kinds of malfunctions, misuses, and improbable conditions have to be considered and tested already in the development phase. There are also other issues to take into account. For example, where microphones and loudspeakers should be installed in the practical confined spaces to achieve the optimum performance.

Like in many development projects, during an ANC application development project it is not often possible or sensible to search for optimal solutions through tests or measurements with real components in a real environment. In some cases, the components or the environment might not exist at all and decisions have to be made with available scant information. In addition, the project teams or consultants doing active noise control design can be situated in some other location and at least a part of the work is preferably done remotely. Measurements are also time-consuming and easily provide a vast amount of data without deeper meaning.

One possible solution for the preceding challenges is to move at least a part of the development process to a virtual environment and simulate instead of measuring. With simulations, it is possible to get more information and test alternatives. There are many highly sophisticated programs for simulations and computers have enough computing power to run useful but rather

complex models at adequate speeds. Simulation tools offer a repeatable and controllable environment in which to test and compare alternatives.

For successful simulations, a proper model of the system of interest is required. With accurate simulation models, it is possible to test the significance of different parameters and find explanations for the observed phenomena more easily than just with measurements. The point when simulations have to be switched to measurements depends on the accuracy of the simulation model. To be able to trust simulation results and to benefit most from the models, we have to know where this point is.

The work presented in this thesis was carried out with funding provided by VTT. The work started to meet a need for a model of a practical active noise control system. Automotive applications have been of interest at VTT and the special focus selected for this thesis was the effects of an ANC system in locations away from error sensors in a confined space. The interest in noise control in locations away from error sensors is related to the fact that in practical systems, the error sensors needed for active control cannot be very close to a passenger's ears. The reasons for that are many, including the limited number of control system inputs, passengers of different sizes, and the need for head movement. In addition, in the automotive applications the noise is not constant. From that perspective, a simulation model capable of correctly simulating situations in which the noise is dynamic was needed.

1.1 Outline of the Thesis

In Chapter 2, a short introduction to active noise control is presented. Starting from the definition of noise, the focus is quickly turned into fundamental parts of an ANC system and control algorithms used in periodic noise control. Also, additional algorithms for active sound profiling and virtual sensing in feedforward active noise control are presented. The emphasis is on the narrowband algorithms that are used in control system presented in Chapter 4. In Chapter 3, models in general and their purposes are discussed and simulation methods for active noise control systems are introduced. In addition, some alternatives for simulations are presented. In Chapter 4, the developed simulation model for a narrowband feedforward active noise control system is introduced and discussed in detail, while in Chapter 5, the output of the model is compared to measurements. Finally, in Chapter 6 the conclusions of the thesis and possible future work are discussed. At the end of the thesis, the measurement data not presented in Chapter 5 is included in Appendix A.

2 Introduction to Active Noise Control

In this chapter, noise control and active noise control systems are presented at a general level. The focus is on the algorithms and methods that are used in the control system to be modelled in Chapter 4. Section 2.1 is an overview of noise control containing both the passive and the active noise control approaches. In Section 2.2, the basics of an ANC system with emphasis on an adaptive filter are presented and in Section 2.3, feedforward control of noise is introduced. Some specific algorithms used in the control system to be simulated are also presented in Section 2.3.

2.1 Noise Control

If sound is annoying or loud enough to damage hearing, it is called *noise* [Kar00]. Noise has many effects on people. In addition to the most obvious, hearing loss, it disturbs speech communication, interferes with sleep, and lowers performance in mental and physical tasks. We can think that noise contaminates us just as any other pollution does. Diminishing noise pollution and its effects on human beings is slowly but steadily attracting more interest. The most straightforward way to get rid of noise is to shut the source off, but that is rarely possible. Noise or sound is often a by-product of a machine or an apparatus and in those cases, the only way to reduce its effects is to try to deaden the noise to an acceptable level. [Ros02]

Conventionally, noise reduction has been implemented with vibration isolators, acoustical absorbing materials, enclosures, barriers, and vibration damping materials. Generally, these approaches to the noise control are a relatively inexpensive way to reduce noise. [Cro97] They are called passive noise control methods because they do not need power to operate. At low frequencies, the noise reduction levels achieved are often inadequate and control of low frequency noise with passive methods only is often impractical as well as costly. For example, mufflers must be large and absorbing walls heavy to reduce noise levels effectively. [Han97]

Fortunately, active noise control can complement passive noise control. The idea behind active noise cancellation is to generate opposite phase sound that destructively interferes with the existing sound field. Active noise control has a broader meaning than just cancellation of noise because the ANC can be used for boosting the desired noise. Active methods are more cost-effective and capable of adapting noise levels at low frequencies, but at higher frequencies of, say, over 500 Hz, complex sound fields and the larger computational load needed in a control

system due to higher sampling rates limits system performance greatly. Comprehensive noise control solutions often combine both of these approaches. [Han01]

Active noise control is a combination of acoustics, signal processing, and mechanics. Although the principles behind active noise control are rather well understood, one has to have a detailed understanding of the limitations and possibilities of those areas to be able to produce a practical application for active noise control. [Ell01] The concept of ANC was patented for the first time in the 1930s, but not until the 1990s did practical implementations became available [Han01]. In the 1990s, control algorithms and the computing power of digital signal processors were developed to a sufficient level to make practical control systems possible [Kuo96]. Nowadays there are not many industrial applications using active noise control, but practical systems can be found, for example, in active headsets, air-conditioning ducts, and propeller aircraft [Ell01].

2.2 Active Noise Control System

The fundamental elements of an active noise control system are depicted in Figure 1. Every ANC system is a combination of electronics and acoustical transducers interacting with the primary acoustic field. Basically, what an ANC system does acoustically is just add a secondary sound field into the existing one. Assuming that these two fields do not interact, we can write the total sound pressure field as

$$p_{tot}(\mathbf{x},t) = p_p(\mathbf{x},t) + p_s(\mathbf{x},t), \tag{1}$$

where subscript p stands for the primary and s for the secondary sound field. Typically, assumption of linearity is valid at sound pressure levels faced in normal situations. [Nel92]

Starting from the electric side, the heart of an active noise control application is a control system that controls the transducers making the secondary sound field. If the control system is self-tuning towards changes in the system under control, it is called adaptive. Non-adaptive systems have fixed parameters and even small changes in the acoustic environment can make non-adaptive system ineffective. An ANC headset is one of the few applications in which non-adaptive control system is workable. [Han01]

The control system is fed with signals containing information about noise. These signals can be either advance signals that hold information of incoming noise, such as a reference signal, or signals that hold information about residual noise, such as an error signal. Not all control systems have a reference signal input. The control system with the reference input is called

feedforward and otherwise feedback controller. Further on, the feedforward control systems are called either broadband or narrowband depending on the type of the noise to be controlled. [Kuo96] Narrowband feedforward control systems are often called also tonal feedforward control systems, and the term is more descriptive, because the noise is periodical and the control approach is slightly different than in the broadband case. The tonal feedforward control is presented in Section 2.3.3.

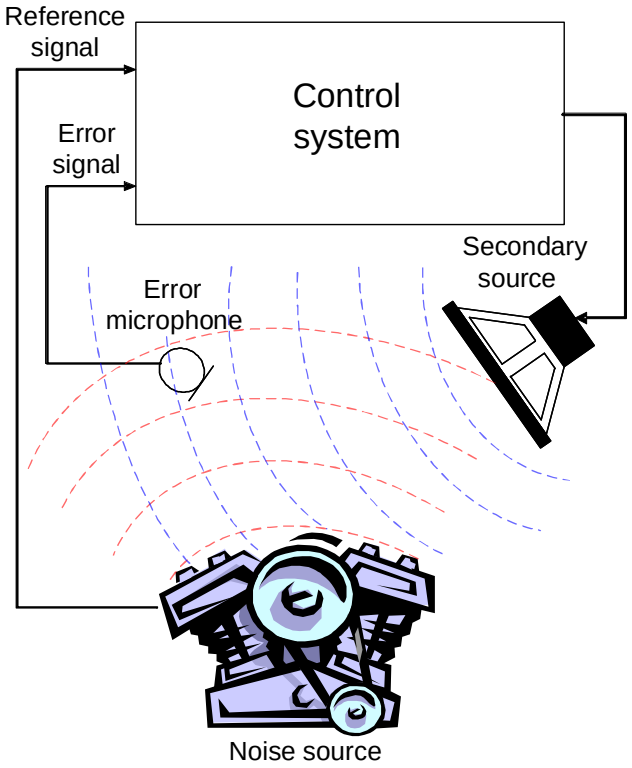

Figure 1. Basic blocks of a feedforward ANC system

The control system output is delivered to a transducer or transducers producing the anti noise. These transducers are often called secondary sources whereas the noise sources, whatever they are, are called primary sources. Commonly, secondary actuators are dynamic loudspeakers, but the secondary noise can be made by any other acoustical transducer as well. For example, in some applications piezoelectric transducers that are attached to a plate are used for transforming an electric signal to sound.

The performance of an active noise control application is dependent on various factors and the factors are more important than others. According to the indicative four-step hierarchy of significances, presented in [Han01], the most important is secondary source arrangement. If the

control sources are placed poorly or they are not capable of producing enough volume displacement, the system will not work properly, no matter how well the other aspects are implemented. In a free space, the control source has to be within the primary source to achieve global noise reduction, but in an enclosed space, the optimal places can be also elsewhere. [Han01] In some cases, the global noise control is not achievable with just a few secondary sources and noise can be controlled only locally. However, local noise reduction that performs well can raise noise levels elsewhere [Ell88].

The second most important factor is the placement of the error sensor. The error sensor has to be placed in the fashion in which it is capable of sensing the relevant parts both of the primary and the secondary sound fields. For example, the modes that the sources of both sound fields excite to the enclosed space. If the control system is of the feedforward type, the next important factor is the reference signal quality. If the reference signal correlates with the error signal to be cancelled, or if there is feedback from the secondary source to the reference sensor, the performance of control is reduced. After all, placing of the transducers and reference signal quality, are optimized, the next important factor to optimize is the control system. [Han01]

2.2.1 Adaptive Filter

Inside of the adaptive noise control system is a digital filter, which is schematically presented in Figure 2. The filter is tuned to filter the incoming reference signal to match the primary noise in a desired way. In fact, the filter is made of two distinct parts, the filter itself and an adaptive algorithm that tunes it. The filter has in most cases a finite impulse response and therefore it is called an FIR filter. Alternatively, filters with an infinite impulse response (IIR filters) can be used. They are able to model more complex systems and feedback with the same computational load as FIR filters. As a downside, the adaptation of IIR filters can converge to a local minimum instead of a global minimum of the optimal filter coefficients space. In addition, the adaptation is slower and more instable. [Han01]

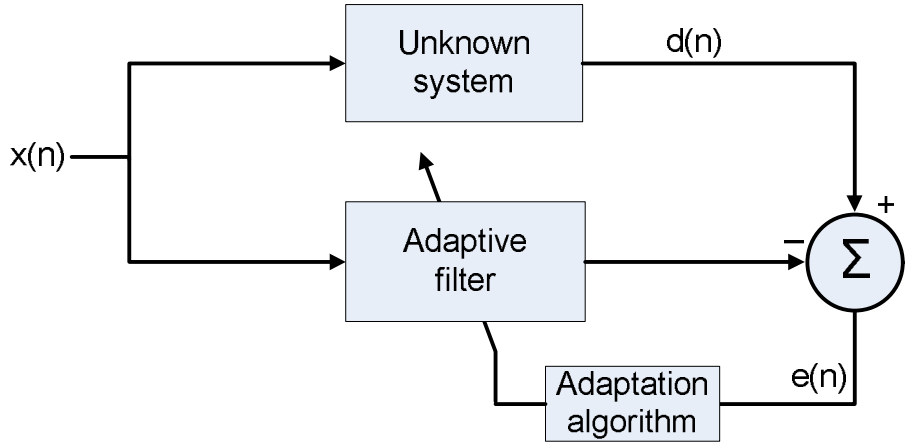

Figure 2. An adaptive filter. x(n) is the reference signal, d(n) is the desired signal and e(n) is the error signal.

It is possible to calculate the optimal FIR filter coefficients to stationary noise using cross-correlation between the reference and the desired signal, marked as *d(n)* in Figure 2, and autocorrelation of the reference signal. The optimal coefficients will minimize the mean square error, MSE, of the error signal. [Kuo96] However, in practical applications with non-stationary noise it is not possible to calculate the optimal filter coefficients from correlation properties of the incoming signals. The computational burden become too great because the optimal filter coefficients have to be calculated constantly. [Ell01]

All the coefficients of an adaptive FIR filter form an $l+1$-dimensional quadratic MSE or performance surface, where l is number of filter coefficients. The surface is 'bowl-shaped' and it has one unique bottom. The theoretical derivation and proof of the existence of the minimum are presented in numerous books, for example in [Kuo96] and [Ell01]. Obviously, in Figure 2, the optimal filter coefficients are exactly the same as in the impulse response of the unknown system. In real situations the surface is time-variant because the set of the optimal filter coefficients do change. There are many methods for adapting FIR filters, and the most widely used one is known as the method of steepest-descent.

In this method, the optimal set of filters coefficients are iteratively searched for following the gradient of the performance surface. In the method, the filter coefficients $\mathbf{w}$ are updated using the equation

$$\mathbf{w}(n+1) = \mathbf{w}(n) - \frac{\mu}{2}\nabla\xi(n), \tag{2}$$

where n is the iteration index, μ is convergence factor or step-size, $\nabla\xi(n)$ is the gradient of the mean square error. [Ell01] The mean square error is defined as

$$\xi(n) = E\left[e^2(n)\right], \tag{3}$$

where $E[\cdot]$ is an expectation value operator and $e(n)$ is an error signal. [Kuo96]

The most commonly used steepest decent algorithm for estimating the performance surface gradient is called *least mean square* or LMS. In it, the value of the mean square error is estimated with the instantaneous value of the error signal. The estimate of the gradient can be solved by calculating the gradient $\frac{\partial e^2(n)}{\partial w(n)}$ knowing that the error signal is

$$e(n) = \mathbf{d}(n) - \mathbf{w}^{\mathrm{T}}(n)\mathbf{x}(n) \tag{4}$$

where $\mathbf{d}(n)$ is the desired signal and $\mathbf{x}(n)$ is the reference signal. Leaving the vector notation, the gradient estimate for each tap w of the adaptive filter is calculated and summed to the old filter coefficient following the equation

$$w_l(n+1) = w_l(n) + \mu x(n-l)e(n), \tag{5}$$

where l is a filter tap index. [Kuo96]

With the convergence factor, it is possible to adjust the convergence speed of the algorithm. If the convergence factor is too large, the adaptation process will become unstable; if it is too small, the adaptation will become ineffective. Indicative limits for the convergence factor are

$$0 < \mu < \frac{2}{LE\left[e^2(n)\right]} \tag{6}$$

where L is filter length. In practice, typically used values for convergence factor are 0.005 to 0.05 times the upper limit of Eq. (6). [Kuo96]

2.3 Feedforward Control

As presented in Section 2.2, as distinct from the feedback controllers, the feedforward controllers have the reference signal input. Basically, in feedforward control, the time that it takes for the noise to propagate from the reference detection point to the error sensor has to be larger than time which the electric control system takes to generate an appropriate secondary sound to the same point. If noise is tonal and its characteristics are slowly varying, the preceding condition can be ignored, but the rate of frequency and amplitude change set the limit

to the validity of the assumption to some point. Almost all of the feedforward control systems are digital. [Han01]

2.3.1 Filtered-reference LMS

In practical feedforward controllers, the situation is slightly different from the ideal situation presented in Figure 2. Between an adaptive filter and an error sensor is a transfer or secondary path. In the ideal case, the optimal filter coefficients, or the transfer function, are the same as in the unknown system, but with the secondary path the optimal filter becomes

$$W(z) = \frac{U(z)}{S(z)} \tag{7}$$

where *U(z)* is the transfer function of the unknown path and *S(z)* is the transfer function of the secondary path. In general, if the delay in the secondary path is greater than in the unknown path, the adaptive filter is non-causal. The other important issue is the possibility that in the secondary path the gain of the transfer function may go to the zero in some frequencies. In that case, the optimal filter will become unstable. For these obvious reasons, the secondary path has to be compensated in some way to successive control. Without compensation in the reference signal going into LMS-algorithm, the convergence of the adaptation process cannot be ensured. [Kuo96]

One possible solution is to modify the adaptation procedure of the filter coefficients presented in Eq. (5). In widely used filtered-reference LMS algorithm, the reference signal fed in the LMS algorithm is filtered with the estimate of the secondary path. The filter coefficient update algorithm in Eq. (5) is updated by replacing $x(n-l)$ with its filtered version $x'(n-l)$. However, the reference signal fed into the adaptive filter is not filtered the estimate of the secondary path. FXLMS algorithm with tonal reference will converge, although slower, while the phase error in the plant model is less than 90 degrees in the frequencies to be controlled. The adaptation process will be almost unaffected if the phase error is less than 45 degrees. [Bou91]

If the secondary path does not change significantly during the adaptation process, it has to be identified only offline, prior to the switch-on of the system. The online identification is needed if changes of the secondary path will produce instability in the adaptation process. For example, in air-ducts for industrial process, the changes in temperature and flow rate can substantially change the secondary paths and cause instability [Ell01].

Offline identification can be carried out with the same algorithms as actual adaptation of control filters. For example, the secondary path can be identified with LMS algorithm, as in Figure 2. [Ell01] Basic procedure of identification is to generate random sequence and drive it through the secondary path and the adaptive filter. The estimate of the unknown secondary path is then calculated gradually from both outgoing and incoming signals, like in Eq. (5) [Kuo96]

2.3.2 Virtual Microphone

In diffuse sound fields, the capability of noise reduction is limited close to the error sensors. As a rule of thumb, reduction over 10 dB can be achieved only in regions whose diameter is under one tenth of the wavelength of noise. Of course, if the secondary source is under half the wavelength distance from the primary source, noise reduction in a wider area is possible. [Ell88] However, the global control of noise is not realistic in most of the practical cases because there are many sources from where the primary noise originates.

Various methods for extending or moving the zone of silence without moving or adding sensors are available. Current virtual sensing strategies are presented, for example, in [Han01]. One motivation in virtual sensing development has been keeping microphones away from ears in practical applications without decrement in noise control capability.

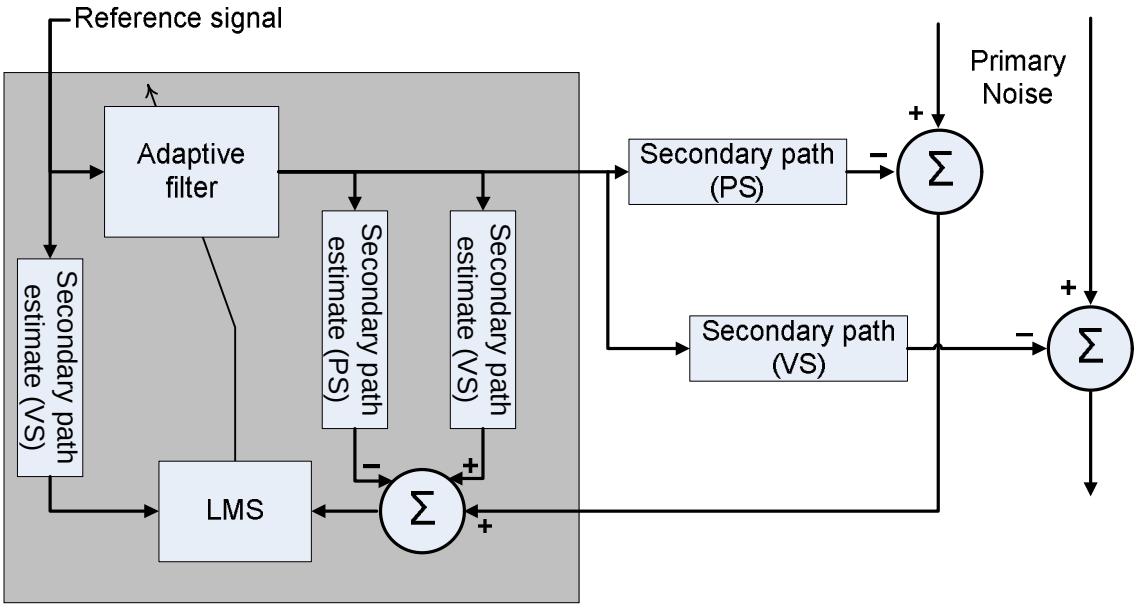

Figure 3. The block diagram of the virtual microphone technique. The acronym VS stands for virtual sensor and PS for physical sensor.

One simple approach to virtual sensing, originally presented in [Ell92], is called virtual microphone. The technique is presented in the block diagram in Figure 3 and it needs an error signal from physical sensor and secondary path estimates both in physical and virtual sensors to be able to estimate the virtual error signal. The primary noise is assumed to be the same in both locations and in a single-channel case is estimated from following equation

$$\hat{p}_p = e_p - \hat{p}_{ps} \tag{8}$$

where circumflex denotes estimate. Error signal estimate in virtual sensor is defined as

$$\hat{e}_v = e_p - \hat{p}_{ps} + \hat{p}_{vs}. \tag{9}$$

Secondary noise component estimates $\hat{p}_{ps}$ and $\hat{p}_{vs}$ physical and virtual sensor location are the outputs of the estimated secondary paths filters. Virtual microphone is a simplification of remote microphone technique [Rou99 & Pop97], in which the transfer function of the primary noise between the physical and virtual sensor is also added in the calculation procedure.

The need for a transfer function from the secondary source to a virtual sensor location limits the practical use of a virtual microphone algorithm. The transfer function has to be determined in some way and in practical applications additional microphones for the path identification do not make sense.

2.3.3 Tonal Feedforward Active Noise Control

If we take a closer look at the noise produced by a fan in an air duct or the engine of a car, we notice that the noise is periodic and related to the speed of rotation. The periodic noise is concentrated in certain frequencies, and in a way, it can be controlled in the frequency domain because each of the harmonics or the orders of the fundamental frequency can be adapted independently. In theory, a single sinusoidal noise component can be controlled with just a two-tap filter, so the computational load is significantly reduced. In practice, more filter weights are needed, usually from 4 to 20 are adequate. [Han01] As a downside, although the lesser filter coefficients reduce the computational load in the adaptation process, the number of filtered reference signals rises if there are many orders to adapt.

The control system in Figure 4 has a tachometric signal as the reference input. For example, in automotive applications the reference signal containing the harmonics of the fundamental frequency is generated inside of the control system from the tachometric signal. The reference sensor can also be acoustical, like in air handling duct applications. But if the reference sensor is

isolated from the secondary source, like the tachometric signal is, the undesired possibility of acoustic feedback from the secondary source to the reference sensor is eliminated [Kuo96].

The reference signal can be generated using the waveform synthesis method. In the method one sampled, complete cycle of the reference signal waveform is stored into the memory. The reference signal is generated by sampling the waveform of the one cycle in a circular fashion. A memory address pointer is increased in every sampling period using the knowledge of the fundamental frequency and sampling time. If the pointer is pointing outside the memory after the increment, the new value of the pointer is calculated inside the memory, taking the remainder of the division with the length of one complete cycle. [Kuo96] If the waveform is sinusoidal, only one-fourth of one cycle needs to be stored in the memory, because the rest of the waveform can be calculated from it. For applications where orders are adapted independently, each of the orders needs its own pointer, but the reference signal can be generated from the same waveform.

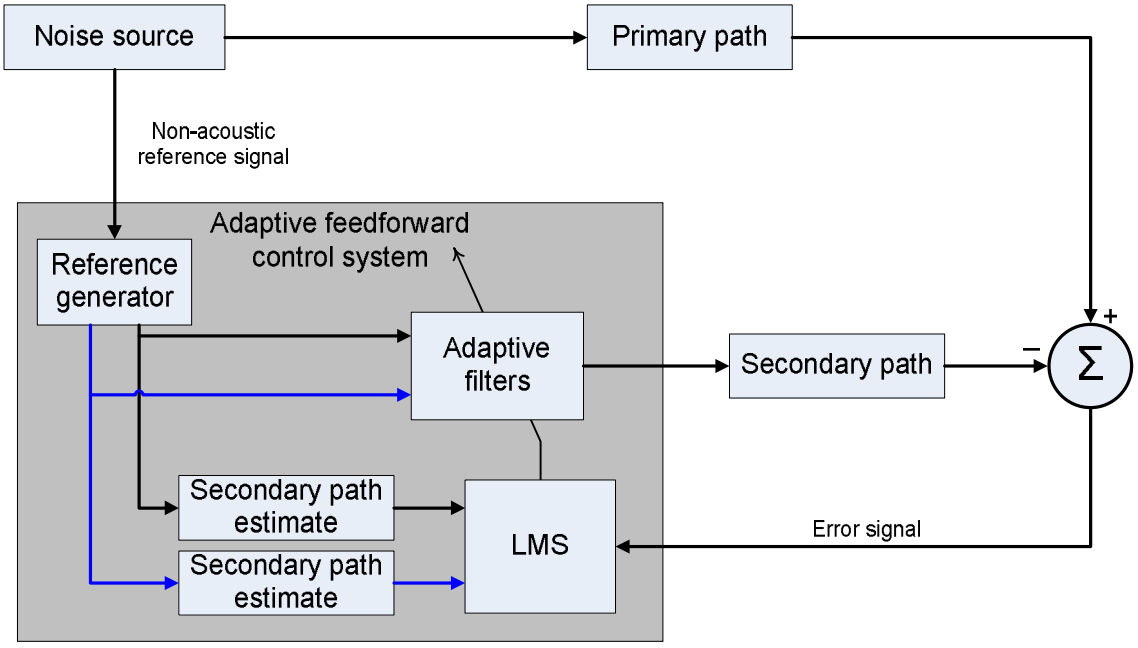

Figure 4. Single channel feedforward ANC system adapting two harmonics of the periodic noise.

2.3.4 Active Noise Profiling

Often by-product sound is considered an unwanted disturbance that should be reduced as much as possible. However, in some application areas, diminishing noise to the minimum is not

preferable. For example, the automotive engine noise is a desired signal that informs and gives impression of quality to the driver. [Mis99] With active noise control systems, it is possible to limit the noise cancellation to a certain limit or even enhance noise to improve the sound quality of noise. Target spectra for the engine sound may be predetermined at different engine speeds. [Ree06] Target values can also be dependent on engine load or gear, for example.

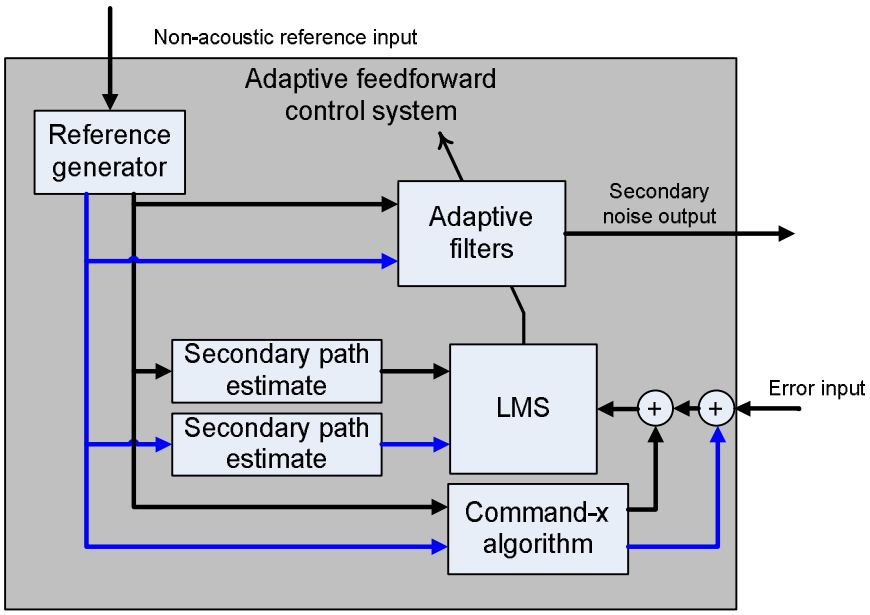

Figure 5. Command-FXLMS.

One stable algorithm for active noise profiling is command-FXLMS, presented in Figure 5. In it, command signal $c(n)$ is made up from the reference signal by weighting each order with target amplitude. Using of the reference signal as input for a command signal ensures the perfect match with the periodic noise components. Error input for FXLMS algorithm is made through substitution

$$e'(n) = e(n) - c(n). \tag{10}$$

where $e'(n)$ is called the pseudoerror signal. Simply, after subtraction the standard FXLMS-algorithm adjusts the pseudoerror signal towards zero. [Ree06]

The needed control effort with the command-FXLMS algorithm is dependent on the phase difference between the disturbance and the command signals. Maximum control effort is needed when the signals are in the opposite phase and minimum when they are in phase. If the signals are in the opposite phase, the control system has to at first attenuate the error signal and then raise the command signal level to the target. [Ree06]

As a simplified example at a spot frequency, if the command signal and error signal are in opposite phase and have the same amplitude, the pseudoerror signal has an amplitude that is double to the original error. The control system sees only the pseudoerror signal and tries to drive it to zero. If we are observing a situation outside the control system, the error signal goes first to zero and then rises back to the initial amplitude but with opposite phase. On the other hand, if the command and error signals are in the same phase and have an equal amplitude, the pseudoerror signal is zero at the start of the adaptation process and the control system has nothing to do.

3 Active Noise Control System Modelling

In this Chapter, different possibilities of modelling an ANC system are presented. In the beginning, in Section 3.1, the concept and some relevant points of modelling in general are presented. In Section 3.2, the modelling of an ANC system is split in two parts, the modelling of the primary and the secondary noise, and both are considered separately.

3.1 Introduction to Modelling

A model is a simplified description of a system or process [Pea02]. Models are more or less simplifications of the reality and they have been used in science for ages. An example of a simple model is Newton's second law of motion, which connects mass, acceleration, and force to each other. The model does not have to be mathematical, but in engineering applications, usually that is the case [Koi07]. The phases of modelling are presented in Figure 6. As can be seen in the diagram, the models can be divided into conceptual and computerized models. The conceptual model is some form of mathematical or verbal presentation of reality and the computerized model implements the conceptual model. [Obe04]

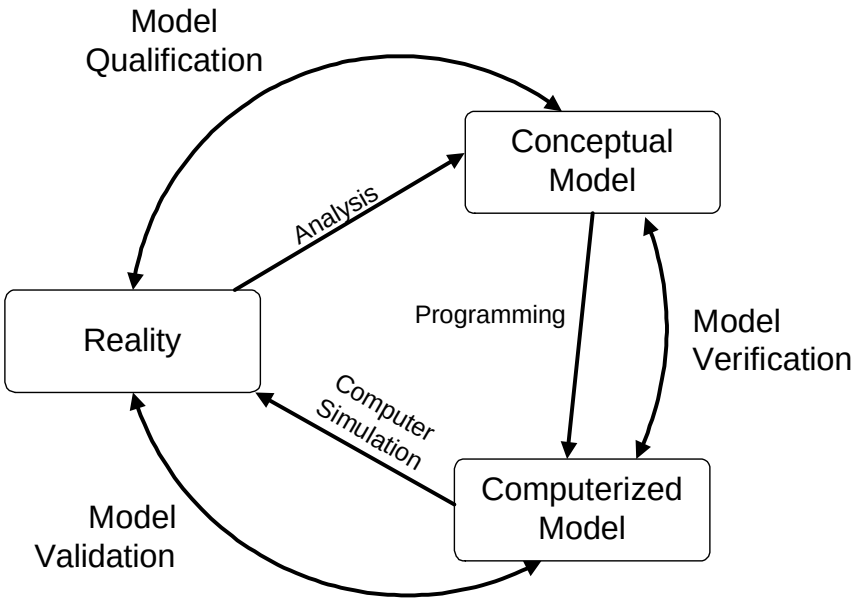

Figure 6. Phases of modelling and simulation. [Sch79]

Before starting to develop a model, one should think first what the purpose of the model is, and keep that in mind throughout the process. Among others, the purpose could be predicting, optimizing or perhaps deepening the understanding of the system. There is not much point using

resources in the modelling of things that are not relevant. Secondly, one should think of the profitability of the model. Traditionally, a product development project was done using practical methods like trial and error because model-based thinking was not familiar. Today, with modern tools, the modelling is more likely to be the cheaper and faster way of achieving good results. Of course, if the purpose of the model is to simulate the hazards of a nuclear plant in an educational simulator, the profitability of the model is not so straightforward. [Koi07]

Thirdly, one should think of the users of the model and how they affect the model characteristics. Is the model going to be a tool for development engineers or a tool for demonstrative and marketing purposes? Fourthly, one should decide how detailed the model should be. For example, if a mechanical model is for designing strengths of parts in static situations, the model can and has to be rather precise. On the other hand, if a model is for designing a control system, a simpler but dynamic model is a better choice. Because of the feedback of control, the simpler model is able to adapt some inaccurateness of the model. [Koi07]

In a simulation, we try to imitate the real system with the model. Although one can simulate models with pencil and paper, nowadays computers are centre-stage in the running of simulations. After the conceptual model is computerized and later verified, it is important to validate the simulation results with the reality. The validation defines the accuracy and reliability of the model.

3.2 Problem-setting

Now, let us turn the focus to the modelling of an active noise control system. The purpose of this thesis was to develop and validate a model of an active noise control system and estimate the effects of the active noise control system in the sound field away from the error sensors. In other words, this meant that the aim was to determine sound pressures in locations other than at the error sensor.

As mentioned in Chapter 2.2, when the active noise control system is switched on, the total sound pressure is a linear sum of primary noise and secondary noise. Therefore, the problem of determining total sound pressure can be divided into two parts, how to determine primary noise, and how to determine secondary noise. The secondary sound field is dependent on the primary sound field at the error sensor locations because the sound pressures at those locations partly

determine the output signals of the control system. In the following two subchapters, the modelling of these two sound fields is approached separately.

3.2.1 Primary Noise

Noise originates from vibrating or moving solid bodies, vibrating air columns, and flowing fluids, for example. [Ros02] Noise sources are seldom point sources and often the noise to be controlled is radiated or transferred to some kind of enclosed space. In the simplest cases, like in the free field conditions or in a rigid walled box with monopole source, the primary sound field can be modelled with analytical functions. A detailed theory of the analytical approach can be found in many constitutive books like [Mor68] and [Fah85].

In analytical techniques, contribution of each element connected to the sound field is explicitly perceivable. Analytical methods are therefore useful for understanding dependencies and origins of noise. However, several challenges arise when the sources and enclosing structures became more realistic. Geometrical shapes, material properties, and forms of construction become complex and easily make modelling challenging and practically impossible. [Fah85] The sound field can also interact with enclosing structures, such as a car cabin or an aircraft fuselage. In these cases, the structural vibration modes excited by outside disturbance and the acoustic modes of interior space couple with each other. [Han01]

One possibility is to use numerical analysis to solve the primary sound field. In numerical methods, continuous field quantities are made discrete in place and time. For example, in well-known finite element analysis, the space is divided into small but finite elements compared to wavelength, and equations are solved iteratively to satisfy limiting conditions. [Fah85] There are numerous powerful programs for simulating sound fields, mechanical structures, and their interaction, but these programs use either with analytical or numerical methods; the understanding of sound radiation mechanisms and parameters of materials and fluids is needed. We also have to remember that modern computers do not have enough computing power to solve all the complex models with all the relevant details, and in some cases the properties of the model have to be reduced.

If the primary noise field exists in real life, one possibility is to measure it. Measuring is easy however complex the sound field is, but the captured sound pressure signals at a finite number of locations do not contain any information about the total sound field around the measurement

points. In addition, measurements are just samples of some unknown distribution without deeper information of the origins of noise.

If noise signals are recorded from a real system, it is important to keep the signals synchronized. It is not possible to get correct results from simulations with more than one sensor location if the noise signals captured in different locations are not in sync. The synchronization can be achieved through simultaneous capture of all channels. If there are many locations where signals have to be captured, it is not always possible to capture all the signals simultaneously. One option is to use a tachometric signal as a synchronization signal. This method is only valid if the primary noise is constant or changes in similar fashion. In Table 2, the benefits and drawbacks of the previous methods are presented.

Table 1. Comparison of methods for determining primary noise. After [Tan95] "Taulukko 15", p. 115.

	Analytical model	**Computational model**	**Measurement**
Low costs	Good	Fair	Poor
Accuracy	Fair	Fair/Good	Good
Generalization	Poor	Fair/Good	Poor
General idea	Good	Fair	Poor
Consideration of details	Poor	Fair	Good

The need and resources determine the appropriate way to model primary noise for simulation purposes. If the need of the simulation is to develop a control system in an existing application, recording noise in suitable locations is an appropriate way to get input for a simulation model. If the whole product is totally in the design phase, using numeric methods for determining the primary noise field might be the only choice.

3.2.2 Secondary Noise

The simulation of the secondary sound field shares the same basic challenges with the primary noise field simulation but has some major differences. Firstly, the sources of the secondary sound field are known better. Secondly, the secondary sources are driven by the control system and one of its inputs is a sum of the primary and the secondary sound fields at the error sensor position. Therefore, simulation of the secondary sound field is recursive and cannot be done independently without the information on the primary noise.

If we are able to measure or otherwise determine transfer functions from the inputs of the secondary sources to error sensors outputs, it is possible to simulate the input of secondary sources with control system model. This includes the assumption that the primary noise is also known. After a simulation, the total secondary sound field can be simulated, because the inputs for the secondary sources are known.

One simple model for estimating a control system is the "ideal" control system, which is a practical approximation if the primary noise is static and there are only one secondary source and error signal. With the method, it is possible to simulate sound pressures at different locations. If we set the total sound pressure, defined in Eq. (1) to zero at the error sensor we come to the equation

$$p_s(\mathbf{x}_e, t) = -p_p(\mathbf{x}_e, t) \tag{11}$$

where $\mathbf{x}_e$ is the error sensor location. On the other hand, the secondary sound pressure at the error sensor is a convolution of the impulse response from the secondary source input to the error sensor and the secondary source input signal

$$p_s(\mathbf{x}_e, t) = h_e * y(t) \tag{12}$$

where h_e is the impulse response of secondary path and $y(t)$ is the input signal to the secondary source. We are interested in knowing the input signal and one possible way to estimate it is to deconvolve it. Taking the Fourier transform $F[\cdot]$ of the both sides of Eq. (12), we get

$$F[p_s(\mathbf{x}_e, t)] = F[h_e] \cdot F[y(t)] \tag{13}$$

and dividing the Fourier transform of the input signal to the left side and taking the inverse Fourier transform $F^{-1}[\cdot]$ of both sides we come to the equation

$$y(t) = F^{-1}\left[\frac{F[-p_p(\mathbf{x}_e, t)]}{H_e(\omega)}\right] \tag{14}$$

where secondary noise is replaced with the right-hand side of Eq. (11) and $H_e(\omega)$ is the Fourier transform of the impulse response. After knowing the input signal for the secondary source we can calculate the estimates of the secondary noise in other than error sensor location. As can be seen in Eq. (14), in the frequencies ω where the Fourier transform of the impulse response goes to the zero, $y(t)$ tends to be infinity. The equation does not limit the input signal

level or take into account the limits of noise attenuation capability, which can result in unrealistic situations. In addition, the assumption of setting the total noise to zero does not take into account what the noise is, e.g. is it broadband or tonal. Of course, it is possible to calculate situations that are more complex, such as putting on more sensors and transducers and limiting the noise reduction to a certain limit.

The noise reduction capability of an ANC system can be estimated with a simple equation that is based on coherence between the reference signal and the noise. With the equation

$$NR(f) = 10 \cdot \lg\left(\frac{1}{1-\gamma^2(f)}\right) \tag{15}$$

it is possible to calculate maximum noise reduction achievable in decibels as a function of frequency. $\gamma^2(f)$ is the coherence function, which can have values between zero to one. For example, background noise in the error sensors will limit the noise reduction capability. If there is more than one error sensor, the estimate of the total performance can be calculated using quadratic optimization. [Han01]

The preceding estimation procedure of ANC reduction capability does ignore the adaptation process and the performance limits of the practical transducers producing the secondary sound field. From that perspective, it seems reasonable to use a more precise model of a control system in a simulation model. A schematic diagram of the basic blocks of an active noise control system in the modelling perspective is shown in Figure 7. For example, delays in the control, algorithms, and their parameters have an effect on the secondary noise. Also, the dynamic properties of the noise have an influence on the secondary noise and therefore the control system cannot be estimated with a simple equation.

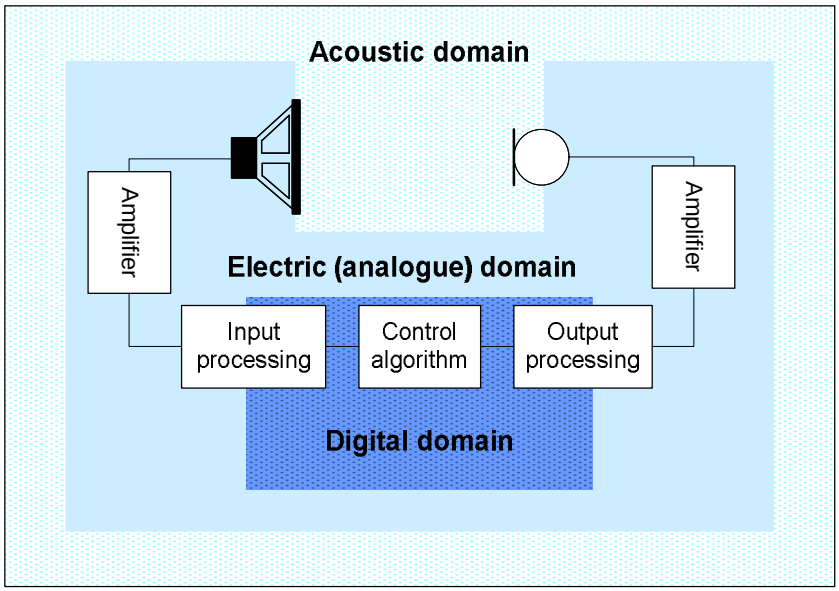

Figure 7. Schematic diagram of an active noise control system blocks.

As a conclusion, there is not much point in simulating the primary sound field simultaneously with the secondary field if the secondary field does not affect the primary field. If the secondary sound field has an effect on the primary sound field, for correct results the simulations have to be carried out by combining the simulations of the primary and secondary noise and control systems.

4 Simulation Model

In this chapter, the simulation model for an ANC system is presented. The system to be simulated and the simulation model are presented briefly in Section 4.1. In Section 4.2, the sampling rate of the model and in Section 4.3, the modelling of the primary noise is explained In Section 4.4, the secondary path models are presented and in Section 4.5, the control system model is introduced. In Section 4.6, the calibration procedure of the model is presented and in Section 4.7, the efficiency of the simulation model is discussed.

4.1 Active Noise Control System Overview

The active noise control system to be simulated was a measurement setup built up for this thesis. The ANC system was idealized compared to the realistic active noise control engineering challenges because the noise was generated with a loudspeaker and therefore it was possible to construct a good reference signal. The idealized situation was considered a more fruitful situation to test how well the simulation model is able to imitate the real world because then it is possible to preclude some sources of uncertainty.

The system to be simulated included two loudspeakers, one for the primary and another for the secondary noise, the control system, three microphones, and a function generator for the tachometric signal. One of the microphones was used as an error sensor and two others were sensing the sound field in other locations. These two sensors were not attached to the control system. The control system was a digital tonal feedforward system with one error and one tachometric input. The basic algorithm code of the control system has been developed at VTT, mainly by Research Scientist Jari Kataja.

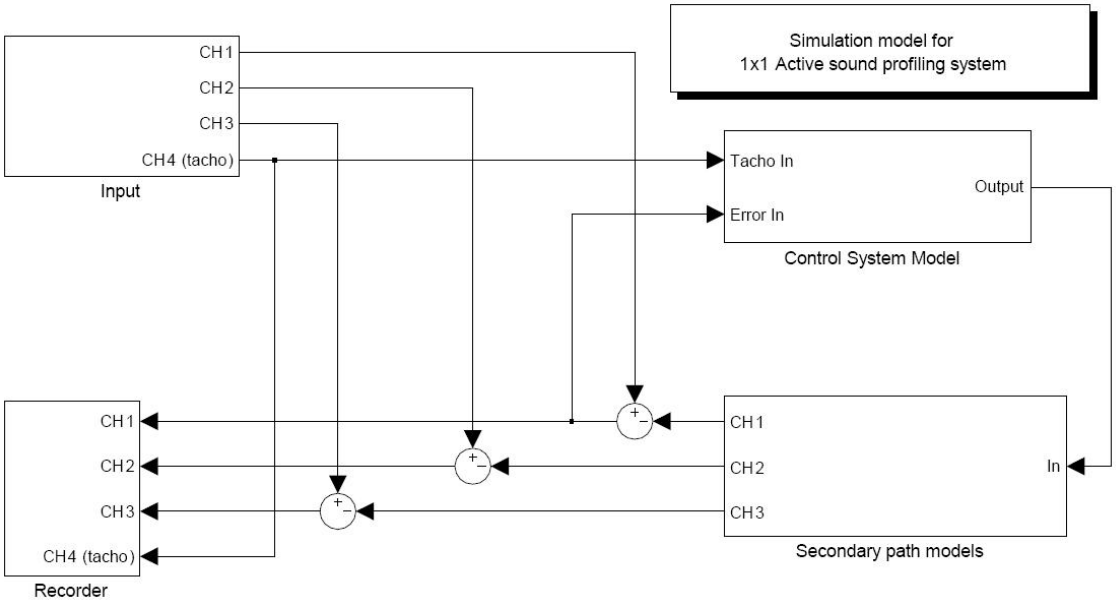

Figure 8. The simulation model at the top level.

The simulation model, which is presented at the top level in Figure 8, was made in a MATLAB Simulink environment. MATLAB is an environment and a technical computing language, which is almost a standard in engineering world. MATLAB Simulink extends basic MATLAB to a graphical environment for model-based simulations. Simulink enables various time domain solvers for models. Simulink is able to solve or simulate models in continuous time but also discrete solvers are available. In addition, it is possible to solve models combining analogue and digital, or hybrid, signals, and models with multirate digital signals. [Mat07]

At the start of the modelling process, the whole system was divided in two sections, a physical plant model and a digital control system model. The line between physical plant and control system was drawn to the enclosing case of the control system. Inputs for the model were from pre-processed files and the outputs of the model were put into audio files.

4.2 Sampling Rate

Digital systems operate with discrete time and amplitude signals that are sampled from analogue signals. Analogue-to-digital and other interfaces in the control system under interest are presented in Figure 9. The lowest possible sampling rate, 8 kHz, for analogue-to-digital converters of the DSP card was selected. However, running the control algorithm at such a sampling rate was not possible due to the computational burden. Also, such high sampling rates are not usually used in active noise control systems. The control algorithm was configured to

run at 1 kHz sampling rate and compulsory decimation and interpolation blocks with low pass filters were added.

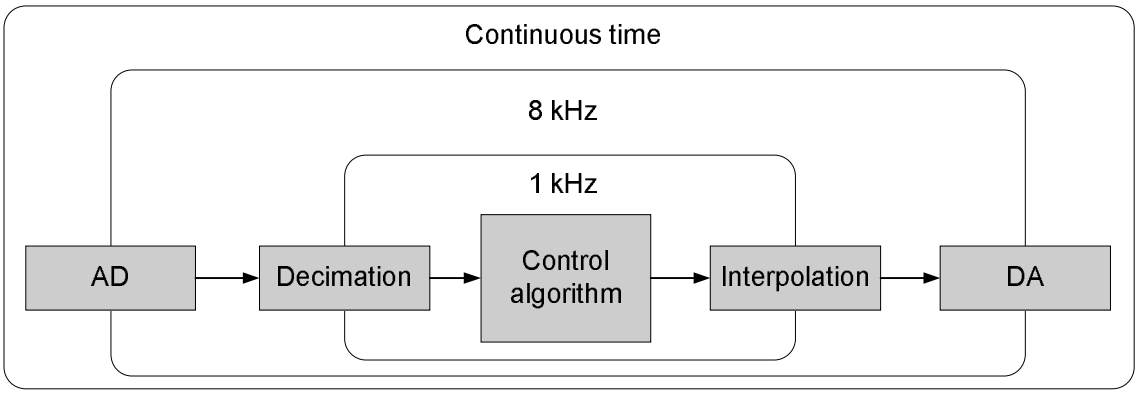

Figure 9. A schematic block diagram of sampling rates of the control system.

In this simulation model, a multirate solver with discrete stepsize running at 8 kHz and 1 kHz was used. The control algorithm was simulated at 1 kHz according to the real implementation of the control system. All other blocks were simulated at the higher sampling rate. The decision was based on the fact that the control algorithm was executed at 1 kHz, which limits the content of the secondary field below 500 Hz. Therefore, the information about primary noise over 4 kHz was discarded. If listening tests of simulations are considered important higher sampling rates might be appropriate. Of course, it is possible to add lost information afterwards simply by adding noise at higher frequencies from the original noise signal to the simulation output files.

4.3 Primary Noise

As mentioned in Section 3.2.1, there are many ways to determine the sound field created by the primary sources. Within the scope of this thesis, the primary noise was interesting only at the sensor locations. Instead of modelling noise sources and the transfer paths to microphones, or modelling the complete noise field, the primary noise field was recorded in all three microphone locations.

The noise recordings from the three microphones and the tachometric signal were captured from measurement setups, presented later in Chapter 5, with a calibrated four-channel measurement system. The sampling rate of the captured files was 12.8 kHz but the files were downsampled in MATLAB to match the sampling rate of the simulation model. The captured signals contained,

in addition to noise to be cancelled, all the background noise outside the control system, so there was no need for additional modelling of the background noise.

4.4 Secondary Paths

The secondary path from the control system output to its error input consists of the acoustical transfer function between the loudspeakers and the microphones, and additional electronics, such as amplifiers. If the path is linear and time invariant, it can be characterised as an impulse response [Sta02]. If the loudspeakers and the microphones or their electronics are not driven to the non-linear range, the assumption of linearity seems realistic but has to be considered.

There are various different measurement techniques for impulse responses, such as the maximum-length sequence or MLS and the sine sweep method. The methods have their benefits and drawbacks. For example, MLS performs nicely in a noisy environment but has to be optimized to obtain optimal results and distortion is included in the result. In this context, optimization means gain adaptation signals. In a quiet environment, the sine sweep method is a better choice because with this method it is possible to remove harmonic distortion from the impulse response and there is no need for tedious optimization. [Sta02]

The secondary paths were modelled from the measurement setups presented in Chapter 5 using white noise. Also, other measurement signals, such as sine sweep and pink noise, were tested, but no major difference between them was found. Both the input and output of the noise were captured and transfer function was estimated with MATLAB function *tfestimate*. The function calculates linear time invariant transfer function using the equation

$$T_{xy}(f) = \frac{P_{xy}(f)}{P_{xx}(f)} \tag{16}$$

where cross power spectral density of the input and the output is divided with the power spectral density on the input. The power spectral densities are calculated with Welch's averaged periodogram method. For more information see [Wel67]. [Mat07]

To reduce risk, the estimated transfer functions were compared to the transfer functions measured with the built-in procedure of the measurement software SIA-Smaart. Then the estimated transfer functions were converted to the impulse responses with inverse fast Fourier transform. Strictly speaking, there was only one secondary path in the simulation model because the system had only one error input. The other two transfer paths from the input of the

secondary source to the output of the microphones were not connected to the control system but used only for observing the sound field.

The entire secondary paths were modelled as single finite impulse responses for each “channel”. It is also possible to split the model of a secondary path into smaller elements, for example, into a model of a loudspeaker and a model of a microphone amplifier. This approach might be beneficial when modelling, for example, for loudspeaker selection.

The secondary path estimate needed for successful control in the FXLMS algorithm was estimated with a separate simulation model for identification only. In the model, the control system contained only the LMS identification algorithm and was connected to the secondary path model from the control system output to the error sensor output. The path was identified for the same duration as the real system. This procedure was used in the calibration of the model as well. The calibration is presented in Section 4.6.

4.5 Digital Control System

The control system platform to be simulated was TMS320C6713 DSK, a DSP Starter Kit card made by Spectrum Digital. The card is a development platform for Texas Instruments’ floating point C67XX digital signal processor family. When operating at 225 MHz, the processor is able to process up to 1350 million floating-point operations per second and 1800 million instructions per second. A block diagram of the signal processing card is in Figure 10. Within the scope of this thesis, the most important parts of the DSP card are the digital signal processor itself and parts that are transferring audio signals in and out of the DSP.

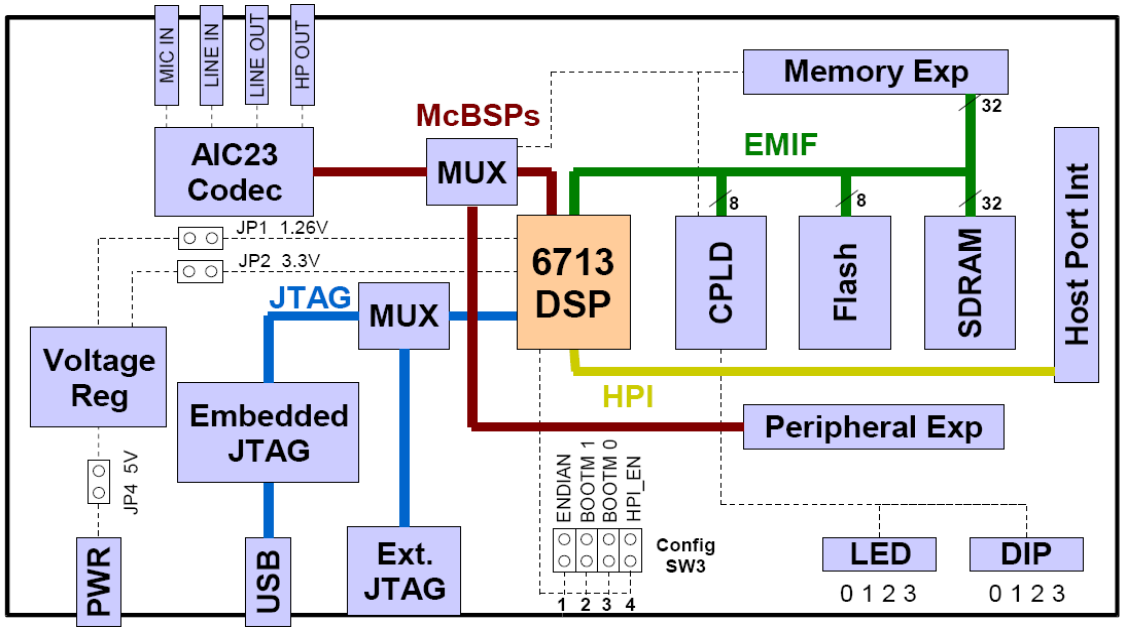

Figure 10. Block diagram of C6713 DSK. From [Spe03], Figure 1-1.

The control algorithm loaded on to the DSP card was an implementation of a single channel narrowband FXLMS algorithm with an additional active noise profiler and a virtual sensing algorithm. The offline identification procedure of the secondary path was also implemented in the control system. As mentioned earlier, in the simulation model the identification was done separately, but it is also possible to add it to the simulation model. In this case, there was no point in identifying the secondary paths because they remained the same between the simulations.

4.5.1 Analogue-to-Digital and Digital-to-Analogue Converters

The control system model is more than just control algorithm implementation. Before the actual DSP, continuous time and amplitude signals are converted in discrete time and amplitude and vice versa after the DSP. The conversions are done by analogue-to-digital (AD) and digital-to-analogue (DA) converters. Their effect on control system performance has to be considered when developing a simulation model. Basically, the converters filter and distort signals, and filtering, in addition to spectral shaping, introduces delay to signals. In this context, distortion means the distortion introduced in the quantization phase. Of course, there might be some non-linear effects in the conversions.

In the signal processor card the converters are in Texas Instruments' high-performance stereo audio codec TVL320AIC23B, which uses multibit sigma-delta technology in AD and DA conversion. [Tex04] Sigma-delta converters oversample incoming signal and they have in-built digital anti-aliasing filters which are optimized for audio use. Filters have low ripple, linear phase response in the passband, and high attenuation in the stop band but also long group delay. In that respect, sigma-delta converters are not optimal for delay-intense applications such as ANC. [Ell01] However, when noise is periodical the delay is not that critical if the noise is slowly varying, as mentioned in Section 2.2.

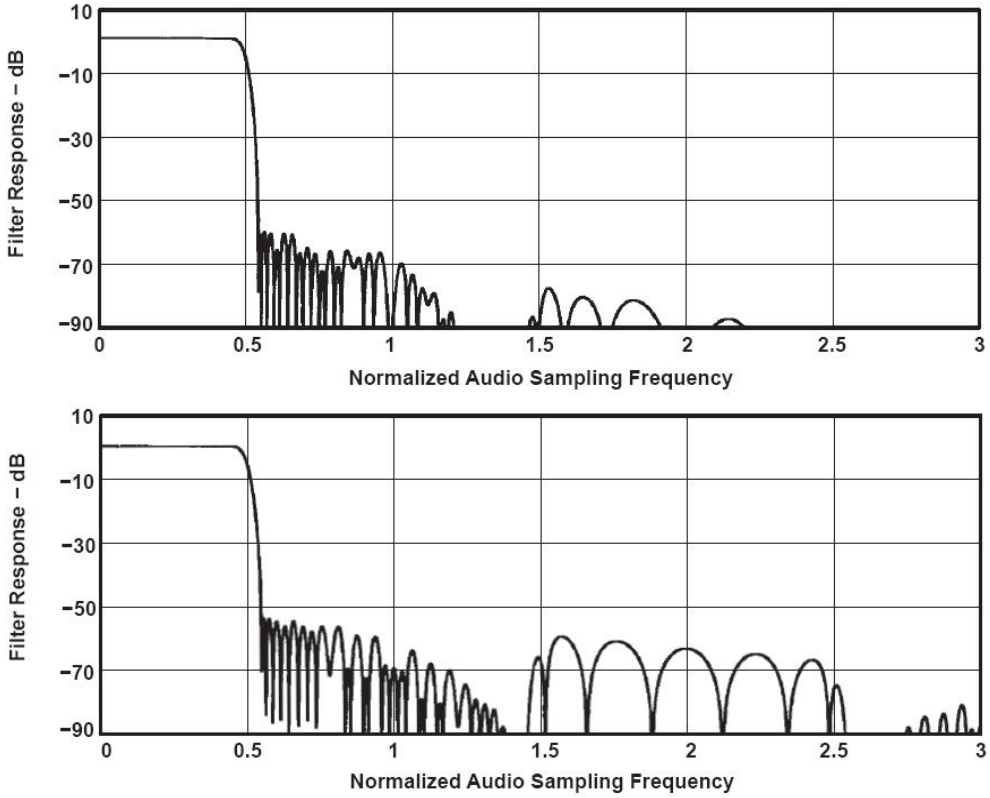

Figure 11. Filter responses of AD-converter (in upper diagram) and DA-converter. From [Tex04], Figures 3-11 and 3-19.

The codec has many different optional lowpass filter responses, which all depend on the selected sampling frequency. In this case, the filters of *type 0* were selected. With that setting, the group delay in the AD converter was reported to be eleven samples and in the DA converter twelve samples, according to the manufacturer. The overall shape of filter magnitude responses can be seen in Figure 11. The peak-to-peak ripples of the magnitude responses in the pass bands were claimed to be below 0.1 dB. [Tex04]

The sampling frequency of the simulation model was selected to match the sampling frequency of the converters, so from that perspective, a reasonable model for converters were just simple delays. Simple delays were good estimates because the magnitude responses of the converters were flat, the frequency content of the signals passing the converters were below 500 Hz, and there was no detailed information about AD or DA filter coefficients.

For accurate simulations, it is preferable to scale input signals amplitudes to match those in real systems. It is convenient to be able to use, for example, the same value of the convergence factor for the LMS algorithm as in the real situation. In addition, possible overflows and precision losses are simulated correctly. In the DSP, there are different options for how signals incoming at AD converter and outgoing at DA converter are scaled. In the real control system, both signals were normalized within a range from -1 to 1 to 16-bit accuracy, and at the DA converter possible overflows were saturated. In the simulation model, a saturation block was added to the model of the DA converter to limit signal values as in the real system. Inside the real system and the simulation model, 32-bit floating-point presentation was used. The DA converter model is presented in Figure 12. A memory block, which is needed to remove the algebraic loop in the MATLAB solving procedure, was put in place as a part of DA-converter model because the memory block is also one sample delay.

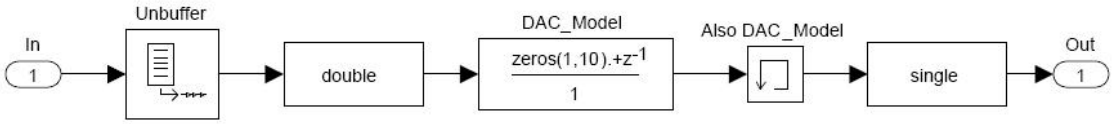

Figure 12. A block diagram of the DA-converter model.

4.5.2 Delays

There was not much explicit information available on the other characteristics of the signal processing card that have to be considered in the scope of the modelling. For example, other delays were estimated and verified through various measurements and comparative simulations. The delays are presented in Table 2. For example, one sample delay at 8 kHz between output channels was discovered with a simple program that summed input signals from two inputs to one output channel. This delay presumably had a very small effect on the simulation result, but the delay was added to the simulation model.

Another more important one sample delay was found at 1 kHz sampling rate. Apparently, the converters of the control system were executed at 8 kHz sampling rate. In reality, the control system was executed at 1 kHz sampling rate because data was compiled in frames at size of eight samples and sent to the DSP. For example, with simple code in which the DSP was just feeding signal through itself, the propagation delay was dependent on the selected frame size.

Table 2. Delays in the control system model.

Source	AD converters	Data transfer in 8 sample blocks	DA converters	Tachometric input
Delay (ms)	1.375 (= 11*0.125)	1	1.5 (=12*0.125)	0.125

Comparison between the real and simulated signal processing card responses is presented in Figure 13. The graphs are made using the identification algorithm that is used in secondary path estimation. In the real system, the output was connected straight to the input with a short wire. The same was done in the simulation model. The impulse responses look a bit different; especially their delays seem to be dissimilar. The frequency domain analysis reveals that the difference in the group delay over most of the frequency range was about half of a millisecond.

In frequency domain analysis, the comparison of the magnitude responses reveals the major difference between the simulation model and the real implementation. In the real system, the total response is highpass filtered. However, it is not evident how the highpass filtering effect is divided between the input and the output. In the simulation model, the highpass filtering was left off. Of course, the left off has some effect to the simulation results, but it was not wanted to guess the place of the filter. On the other hand, with two FIR filters that have group delays of 11 and 12, it is not possible to implement such highpass filtering effect. One possibility for the highpass filtering effect is that there are galvanic decouplers in the input and the output of the DSP card. However, in the simulation results the effect of the absence of the highpass filter is negligible because the lowest frequency of the primary noise was 50 Hz.

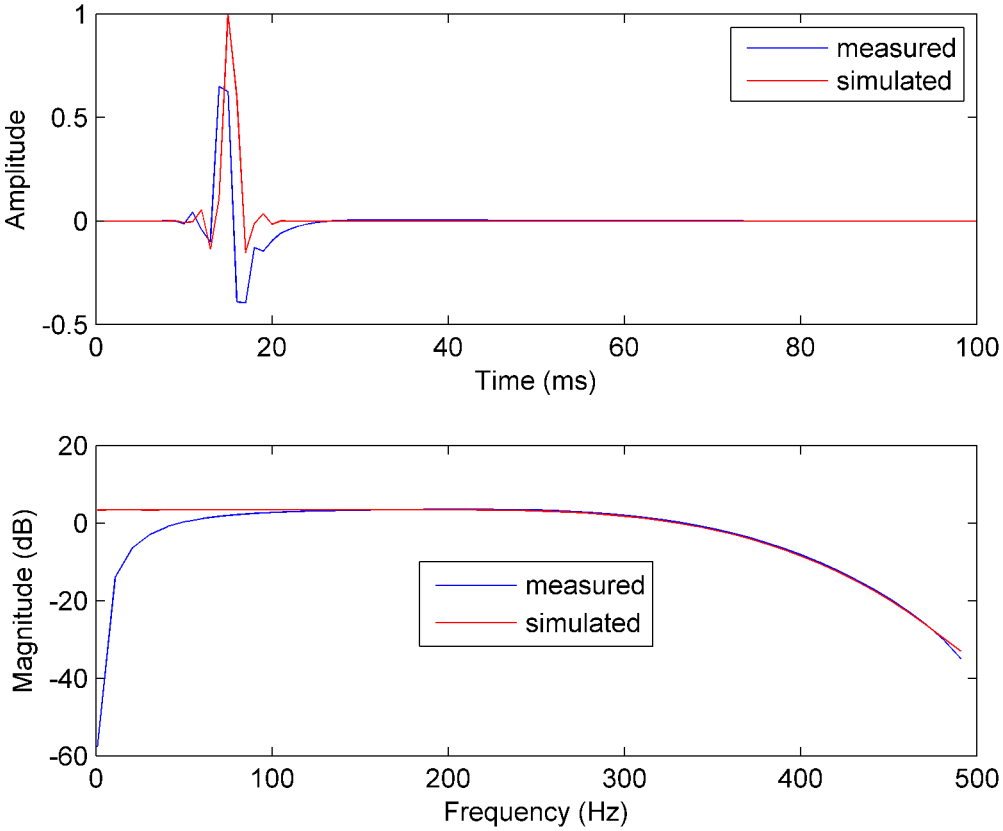

Figure 13. Measured and simulated impulse responses and magnitude responses of the DSP card. The responses are set approximately at equal level in the magnitude domain.

4.6 Calibration

To be able to get accurate and realistic output from the simulation model, it is essential to calibrate the model carefully. In this context, calibration meant adapting gains for every signal replayed from file and secondary noise filtered through the secondary paths to the level that they were equal to the real situation. The input signals for the control system in the simulation model were sums of the primary and the secondary noise.

The model was calibrated using comparative simulations and measurements of the actual control system. The primary noise level was calibrated using information about input signal sound pressure versus the numerical value. A sinusoidal 1 kHz tone, which had sound pressure of one Pascal at measurement microphone, induced a peak value of 0.024 after the AD converter. To be more precise, the corresponding voltage level in the input of the signal

processing card was 54 mV. The relation between sound pressure and numerical value is dependent on the microphone and its amplifier. The sensitivity of each individual measurement microphone is a bit different and, for example, the difference of 3 mV, which is within normal range, introduces change of about 5% after the AD converter when compared to 54 mV.

In the simulations, the calibrated noise recordings were stored as sound pressure signals in the measurement software. The recordings were just scaled down by factor of 0.024 to get correct numerical values after ADC. However, in most of the real situations, the microphones connected to the control system are not calibrated before the control system. In those cases, it might be necessary to add a calibration routine inside the real control system, which takes into account all sensors individually. We have also to remember that small changes in gains do not have a significant effect if we are interested in sound pressure levels, but inside the control system model, the right signal values are more important.

The secondary paths were calibrated with the identification algorithm of the control system. The secondary paths contained AD and DA converters and the transfer function from the control system output to the sensor output in the error channel and in the other two channels only the transfer function. The secondary path estimated from the error channel with the real system was compared to the estimate in the simulation model. Secondary path gain was adjusted in the simulation model until the magnitude responses were at approximately equal level. The iterated gain was applied also in the two other channels. Exact calibration was not possible because the secondary paths of the error channel in the real measurement and in the simulation were slightly different.

With the preceding procedure, it is not possible to split the gain into each of the elements of the secondary path. Concentrating the gain at one spot in the secondary path had no downsides because the values outside of sensors were not of interest. The only concern was to keep the signals entering the control system in the correct order. In that respect, the gain for the secondary paths was inserted before the summing node of the primary and secondary noises.

4.7 Computational Efficiency of the Simulation Model

How fast simulations can be carried out significantly determines the usability of the simulation model. Current computers have lots of computing power, but their limits can be reached even with rather simple models. For example, the time used in the simulations was something from

six to ten times the duration of the simulation signals. The simulations were carried out on an ordinary laptop computer, which was a Dell D620 computer with Intel's Core 2 Duo T5600 processor and 2 GB RAM.

The Simulink environment provides tools to analyze the performance of models and to accelerate them. A report from the in-built profiler revealed that almost half of the time used in simulations was spent in one of the control system blocks that had a large, constantly fetched data table. In future simulation models, the block can be executed faster if it is implemented more efficiently by moving the data table inside the block. All other blocks were rather fast to simulate. For example, each of the secondary path filters took only about 6 percent of simulation time each. As a cautionary note, one should avoid straightforward conclusions about code performance in DSP, because code executed in Simulink models does not behave similarly in DSP. A common example of that is the performance of *for*-loops in MATLAB versus C. For code optimization, at least a simple simulator of the DSP card is needed.

It is possible to accelerate the execution speed of models in Simulink. Basically, the idea behind accelerating is to replace the normal interpreted code with compiled target code. In the current release of MATLAB, R2007b, there are two different acceleration modes. [Mat07] Both of them were tested, but were found unhelpful because the time required for code generation was long compared to saving in simulation time. In addition, code had to be generated every time for every simulation run because names of input and output files were different.

5 Validation of Simulation Model

In this chapter, the simulation model described in Chapter 4 is validated and compared against the results of the two separate measurements cases. The two cases were first measured and then simulated with the simulation model. In Section 5.1, general measurement setups and analysis methods are introduced and in Section 5.2, the programming environment used in DSP programming is overviewed. In sections 5.3 and 5.4, two measured cases are described, analyzed, and compared with the simulations in detail.

5.1 Measurements Overview

A schematic diagram of the measurement setups is presented in Figure 14. Overall, the measurement setups consisted of one Genelec 1029A active loudspeaker making the primary noise and another making the secondary noise, three Brüel & Kjær type 4189 half-inch free-field microphones, the control system and an Agilent 33120A function generator for generating sinusoidal tachometric input signal. The microphones were connected to Brüel & Kjær type 2671 ICP preamplifiers and further on to a PCB Piezotronics signal conditioner for ICP sensors model 482A22. The signals from the signal conditioner were delivered to the control system and a 01dB-Metravib four-channel Harmonie measurement system used for the recordings. The measurement system and the DSP card running the control system were connected to a laptop.

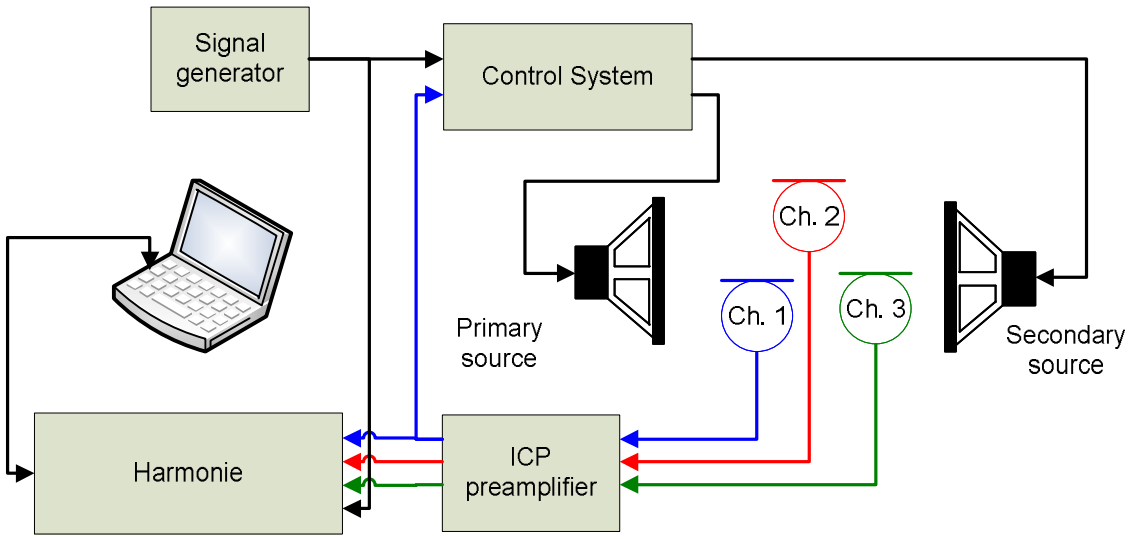

Figure 14. A diagram of the measurement setups.

Both the primary and the secondary noise were made by the control system. The reference signal needed for the FXLMS algorithm that was generated inside the control system from the tachometric input, was also directed to the free output of the signal processing card. In a way, with this procedure the match between frequencies of the noise and the reference signal was almost ideal. In the measurements, the periodic noise components corresponding to the tachometric signal had monotonically increasing frequency from starting frequency to target frequency. The procedure in which the operating frequency is changed constantly is called commonly as run-up or run-down depending on the direction of change. With run-ups, it is possible to find the orders or the harmonic components of the fundamental frequency.

For the simulations, all the microphone channels and the tachometric signal were captured synchronously using the calibrated measurement system. The noise recordings for the simulations included the reference signal and noise from every sensor, so the signal contained all background noise outside the control system. The signals from the sensors were captured as pressure signals, so the later calibration of the simulation model was straightforward. The captured tachometric signal from the function generator was a sinusoidal voltage signal. At the the start of each noise recording there was a few seconds of noise at constant frequency and then the linear run-up to the target frequency. These run-ups, both with actual measurement and with simulation, were analyzed using 01dB-Metravib dBFA Suite software. The only difference was that the simulated recordings were replayed through a USB sound card instead of a proper measurement card. Nevertheless, the measurement chains were calibrated and tested carefully in both cases.

As mentioned earlier, the orders are harmonics of fundamental operating frequency of a rotating machine, for example. It is general practice to analyze systems producing periodical components by tracking orders as a function of rotational speed. It is possible to use the information of the fundamental frequency or the tachometric signal. A typical way to extract order spectrum is to calculate discrete Fourier transform at constant rotational speed intervals. However, if the DFT is calculated over a constant time period, the rapid changes in speed of rotation within one block would produce smearing of the components that are related to the rotational speed. On the other hand, the effects that are not related to the rotational speed, like resonances, are mapped correctly. [Bra05 & dBF04] An example of order extraction is presented in Figure 15. Each order is presented as an increasing straight line and the higher the order, the greater the slope.

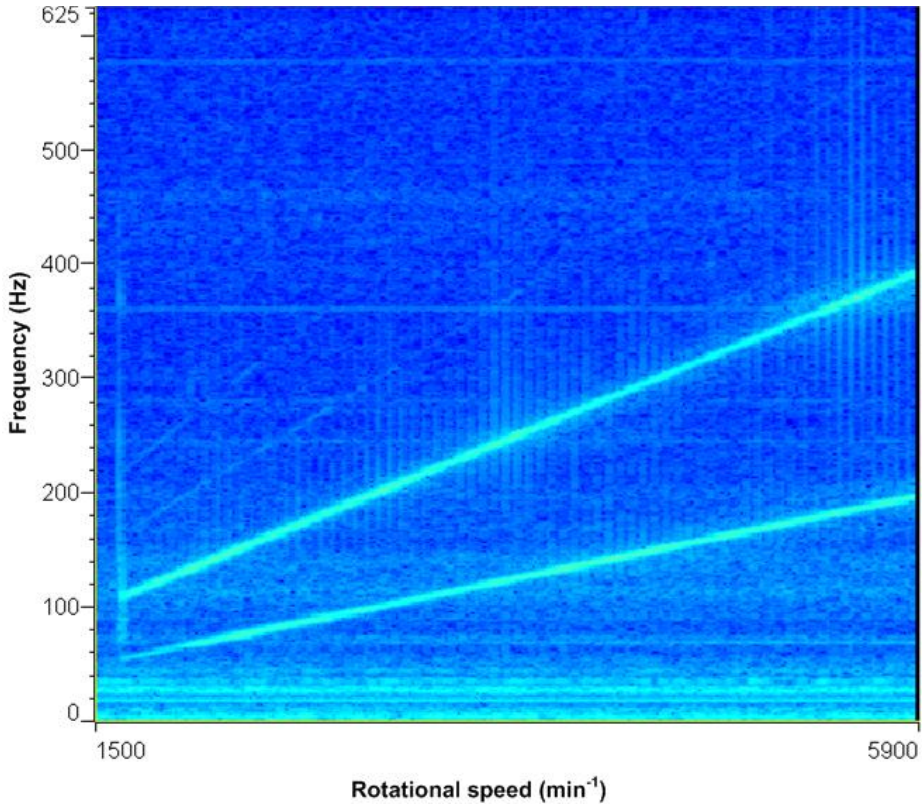

Figure 15. An example of order analysis from a run-up. The sound pressure level is expressed with different colours. Increasing straight lines are the second (lower) and the fourth orders (higher). The non-rpm-related noise components are seen as horizontal lines.

If periodical effects are of interest, there are more suitable methods for order tracking. For example, a method called *RPM-synchronous order tracking*, which was used in analysis of the following measurements. In order tracking with resampling technique, the signal, originally sampled in time domain, is resampled in rotation angle domain. The DFT has constant length in angle domain, but is obviously shorter in time when the rotation speed increases. The benefit of the resampling technique is that the order resolution remains constant throughout the measurement. The order tracking method was built in the measurement software and called *DFT/Resampling* method. [Bra05 & dBF04] The following measurement results are presented in sound pressure levels of a single order as a function of revolutions per minute.

Standard deviations presented in the measurement results are calculated using the formula

$$s = \left[\frac{1}{n-1} \sum_{i=1}^{n} (x_i - \bar{x})^2 \right]^{\frac{1}{2}} \tag{17}$$

where

$$\bar{x} = \frac{1}{n} \sum_{i=1}^{n} x_i \, . \tag{18}$$

The duration of the secondary path impulse responses used in the simulation model were approximately 0.6 second. The lengths of the impulse responses were relatively short, but after 0.6 second the level of impulse responses amplitudes were decreased more than 60 dB. Longer impulse responses made no significant difference in the simulation result.

5.2 Programming Environment

Like the simulation model, the program code for the real system was made in a MATLAB Simulink environment. From MATLAB the model was converted to DSP through Code Composer Studio, an integrated development environment for TI's digital signal processors. Simulink and Code Composer studio were connected to each other with MATLAB's Link for Code Composer Studio. The procedure used in programming is illustrated in Figure 16.

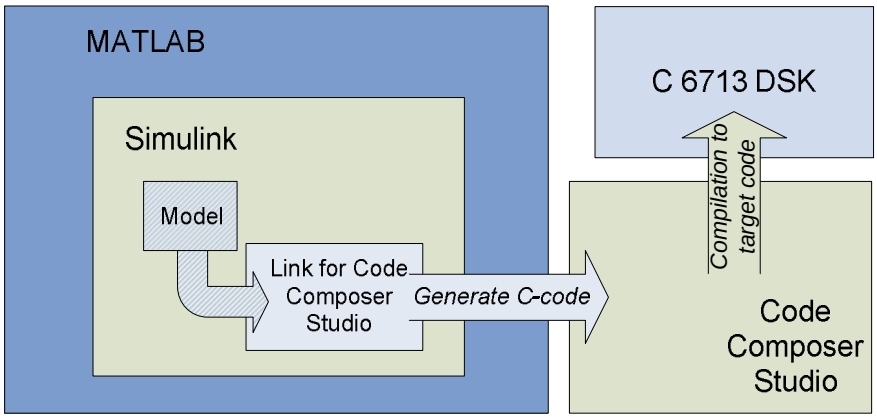

Figure 16. The concept of code generation from Simulink to DSP.

Basically, with the procedure one can develop and test signal processing applications in the Simulink environment and then generate ready-to-use code for DSP through Code Composer Studio. In this case, the control system model was taken from the simulation model presented in Figure 8, and the AD and DA converters were replaced with blocks that were in the Simulink library.

5.3 Measurement with Control System Using Active Noise Profiling

In the first measurement, the control system was configured to adapt noise to a constant level instead of minimizing it. The used active noise profiling algorithm was very simple: the target level for both orders was 50 dB throughout the RPM range. The profiler was implemented with command-FXLMS algorithm introduced in Section 2.3.4.

The measurement setup was erected in the corner of a large room. Room dimensions were 2.8 m by 14.0 m by 5.5 m and all parts of the measurement setup were more than one metre away from walls. The walls and the ceiling were damped with 50 mm absorbing material and the floor was covered with vinyl flooring. Pictures of the setup are presented in Figure 17 and Figure 18. The reference axes of the loudspeakers were 1.45 m from the floor and faced each other. The distance between loudspeakers was 1.2 m. The microphones were placed between the loudspeakers in a rather large formation where the first microphone, Ch. 1, was used as the error sensor. It was placed 0.45 m from the secondary source along its references axis. The second microphone, Ch. 2, was placed 0.5 m from the primary source at a height of 1.2 m. The third microphone, Ch. 3, was put very close to the secondary source, at a distance of 0.2 m.

The primary noise consisted of two sinusoidal tones that were the second and the fourth orders of the fundamental frequency. The tachometric signal was a 30-second long linear sweep from 1500 min^{-1} to 6600 min^{-1}, corresponding to frequencies from 25 Hz to 110 Hz, so the second order was between 50 Hz and 220 Hz and the fourth order between 100 Hz and 440 Hz.

Figure 17. The first measurement setup. The primary noise source is on the left and the secondary noise source on the right. Microphone locations are circled.

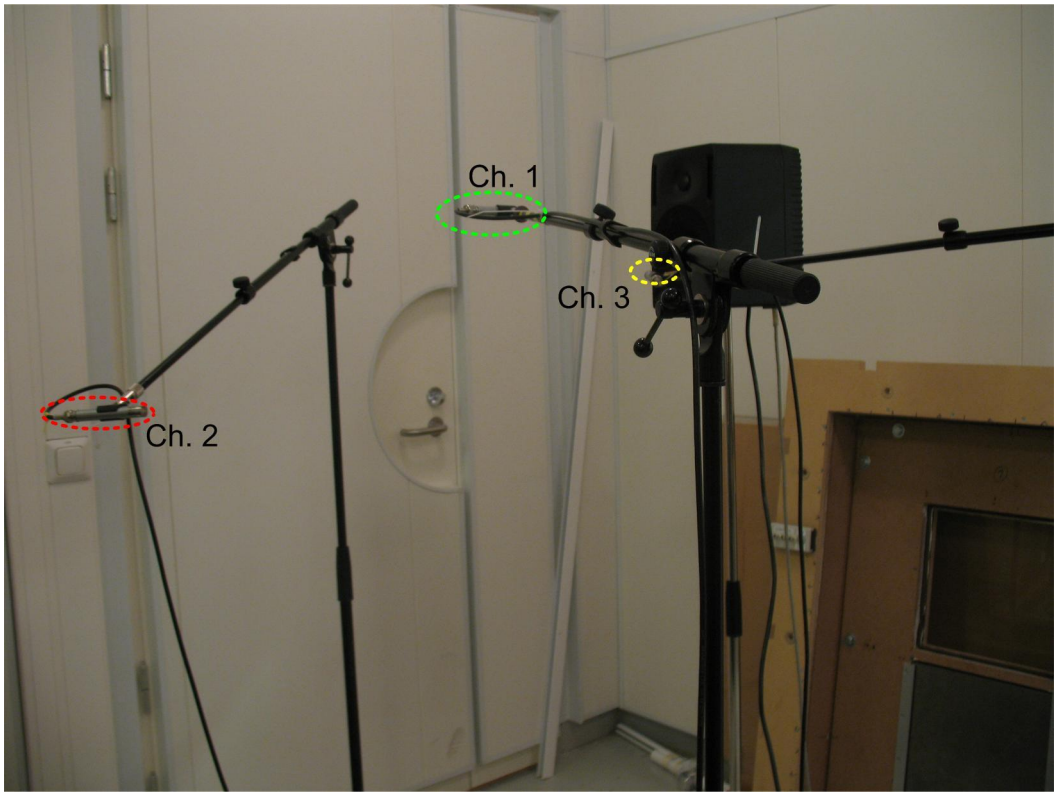

Figure 18. The first measurement setup from a different viewpoint. Microphone locations are circled.

The results of the simulations and the measurements with the control system are partly presented in Figure 19 throughFigure 21. The rest of the processed measurement data can be found in Appendix A. The averages and the standard deviations in the measurement results of the primary noise and the simulations were taken from ten measurements. One of the run-ups with ANC on was discarded because adaptation became unstable at the end of the run-up. The averages and the standard deviations with only the primary noise on are shown to give the understanding of the performance of the control system.

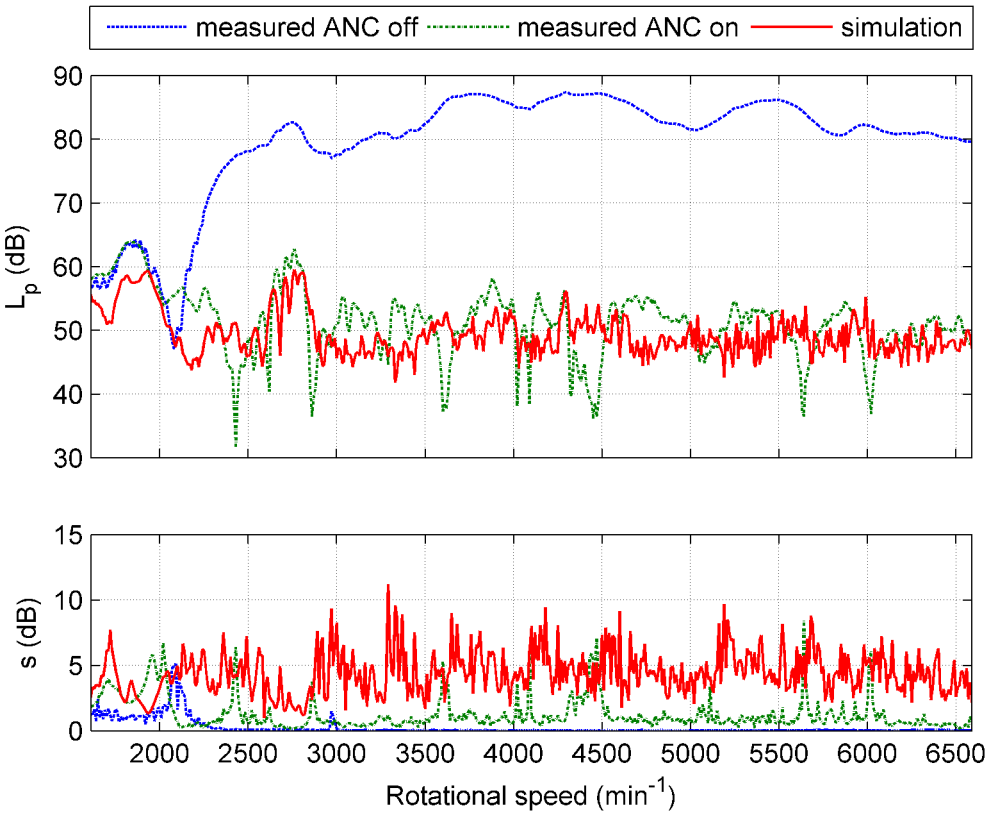

Figure 19. Averages and standard deviations of sound pressure levels of the second order at the error microphone (Ch. 1) location. The target value for the active sound profiling was 50 dB throughout the frequency range.

As can be seen in the graphs in Figure 19 and Figure 20, in the run-up measurements with ANX on the achieved sound pressure level varies around the target value, but in separate tests with static noise, which are not presented here, the control system was able to achieve the target value of sound pressure level well. The wiggling around the target value is an example of the adaptation process. In Figure 19, the simulation of the second order traces the measurement weakly in the error sensor location, but the fourth order, in Figure 20, matches better. The rise at the sound pressure levels of the fourth order is at least partly due to the effect of the interpolation and the decimation filters. The low pass filtering effect of those filters can be seen in Figure 13.

Although the measured green line looks random, the standard deviation of ten measurements is mainly one or two decibels, so in the measurements the adaptation process of the control system

was reproducible. The high peaks in the standard deviation correspond to the valleys on average. The depth of the troughs was different in each of the measurements probably due to the background noise.

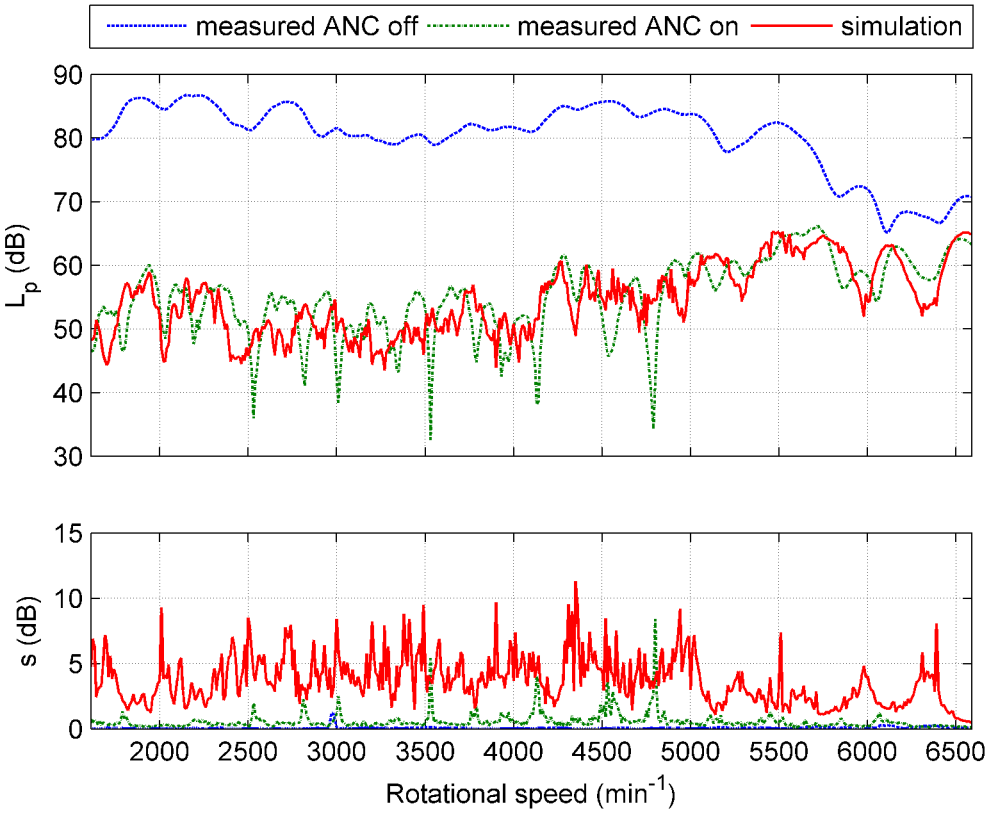

Figure 20. Averages and standard deviations of sound pressure levels of the fourth order as a function of rotational speed in the error microphone (Ch. 1) location. The target value for the active sound profiling was 50 dB throughout the frequency range.

In the error sensor location, the standard deviation of simulations is significantly bigger than in measurements. On average, it is approximately five decibels. At the other microphone positions, Ch. 2 near the primary loudspeaker and Ch. 3 near the secondary one, the correspondences are much better. For example in Figure 21, the standard deviations of Ch. 3 are almost the same in measured and simulated situation. The differences between measured and simulated averages of sound pressure levels can be explained for example with differences in the secondary paths and other imperfections, but the greater standard deviations in the simulations are interesting. If the secondary path models are significantly different, the dynamic adaptation process will follow

some other path, but the standard deviation of the different measurement setups should not be different.

Obviously, the first reason for a larger standard deviation is that the model of the control system is not working as it should be. On the other hand, the third microphone was closest to the secondary source so the effect of a wrongly functioning control system should be largest there but, as can be seen in Figure 21, the correspondence between measurements and simulations is good at the third microphone location. The more likely explanation, at least for part of the high standard deviation, is in the analysis procedure. In the analysis of the simulations the wav-files made in the simulation model were played through the USB sound card. Although the measurement system was calibrated carefully, the background noise in the measurement chain was affecting the measurement results. In Figure 20, it can be seen that the rise in the sound pressure level at the end of the run-up slightly reduces the standard deviation. However, if the assumed random component in the analysis phase is truly random, the average of the ten simulations should not be biased very much, so there is a difference between the results of the measured and the simulated cases.

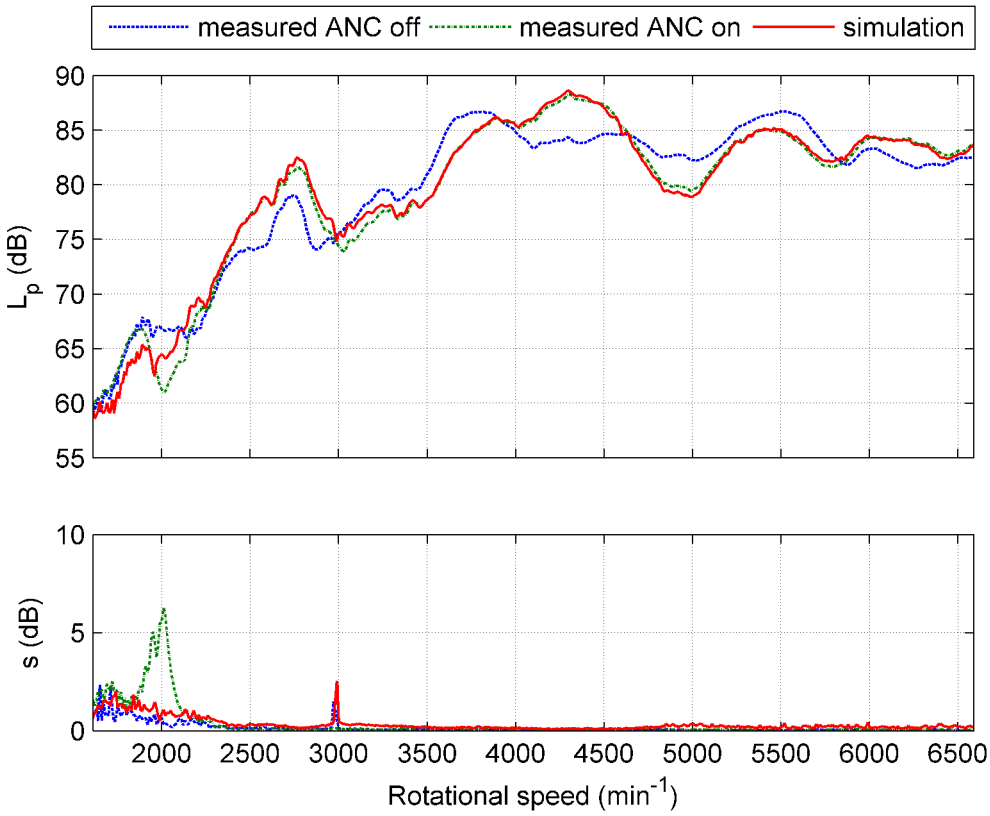

Figure 21. Averages and standard deviations of sound pressure levels of the second order as a function of rotational in the Ch. 3 location.

5.4 Measurement with Control System Using Virtual Microphone

In the second measurement, the virtual microphone algorithm described in Chapter 2.3.2 was added and the active sound profiling block was removed from the control system. The secondary path to the virtual sensor location needed for the algorithm was measured beforehand and implemented into the control system code. The secondary path to the physical sensor location was identified with a built-in procedure as in the previous measurement.

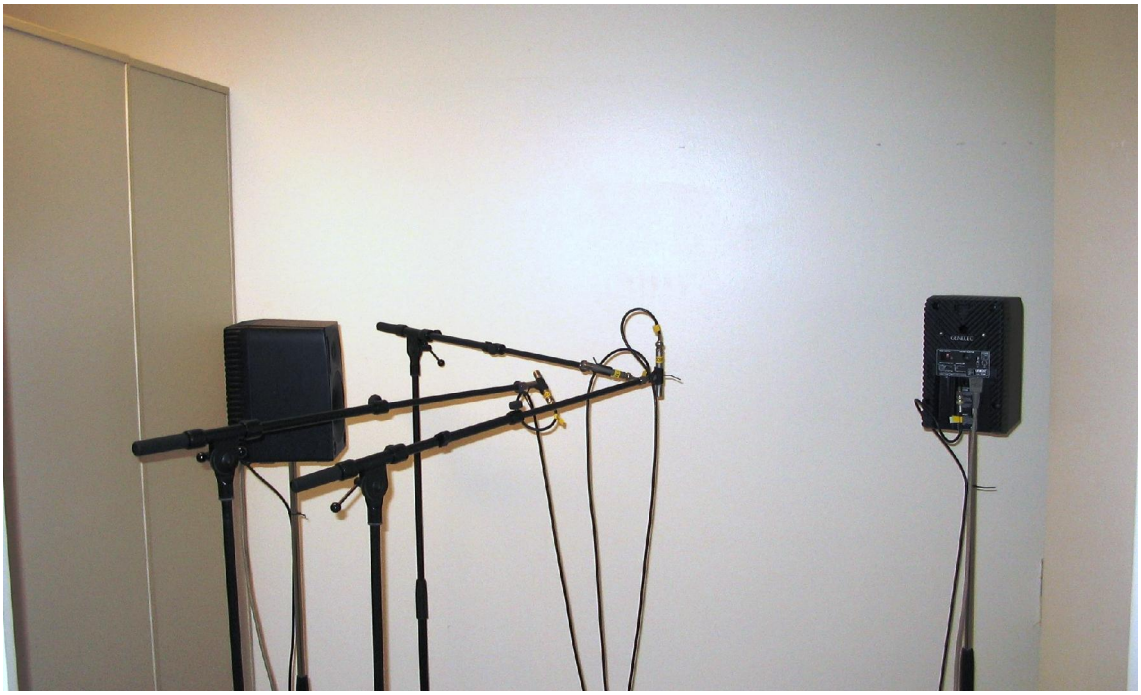

Figure 22. A picture of the second measurement setup. Noise source is on the right.

The measurement setup was erected in a medium-sized hard-walled room with total dimensions 2.9 m by 5.6 m by 4.8 m, but the free space was confined around the setup to 1.6 m wide with bookshelves that were 2.1 m high and 2.9 m long. Obviously, the acoustical environment was more reverberant than in the measurement presented in Chapter 5.3. The pictures of the setup are presented in Figure 22 and Figure 23. The reference axes of the loudspeakers were 1.45 m from floor. The secondary loudspeaker was faced towards the microphone array and the primary loudspeaker was faced towards the corner of the room. The microphones were placed in compact array at the same height as the loudspeakers. The distances between microphones were from 9 cm to 24 cm. The second microphone was nearest to the secondary loudspeaker and the third was nearest to the primary loudspeaker. The array was on average nearer to the secondary loudspeaker than the primary one.

Noise had same orders as in the previous measurement but the tachometric input for the control system was a 40-second linear sinusoidal sweep from 1800 min^{-1} to 6600 min^{-1}, corresponding to frequencies from 30 Hz to 110 Hz, so the second order was from 60 Hz to 220 Hz and the fourth order from 120 Hz to 440 Hz.

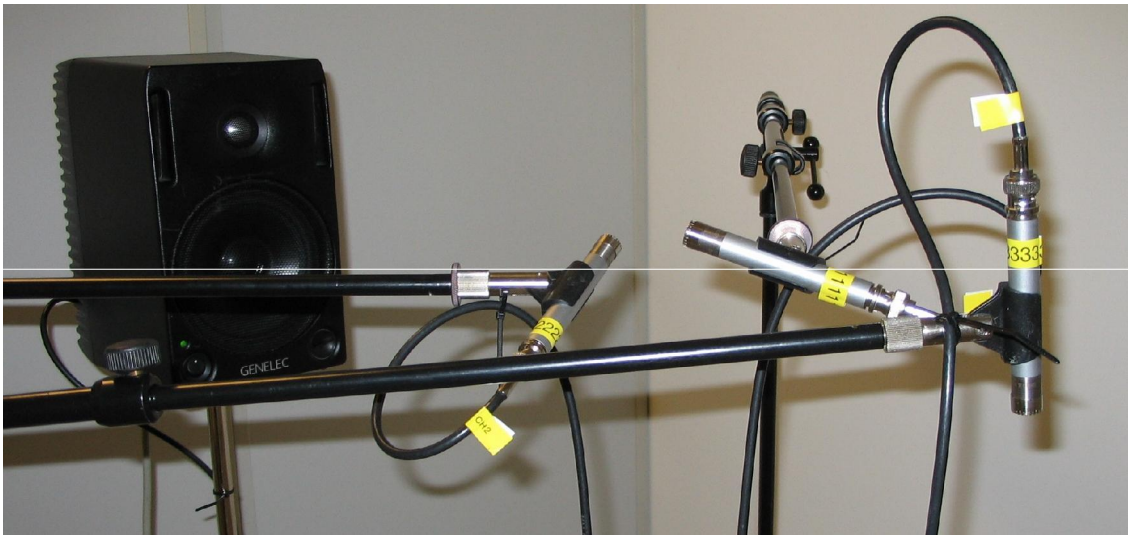

Figure 23. A close-up picture of the positions of the microphones in the second measurement setup. Microphone channels can be seen on the preamplifiers.

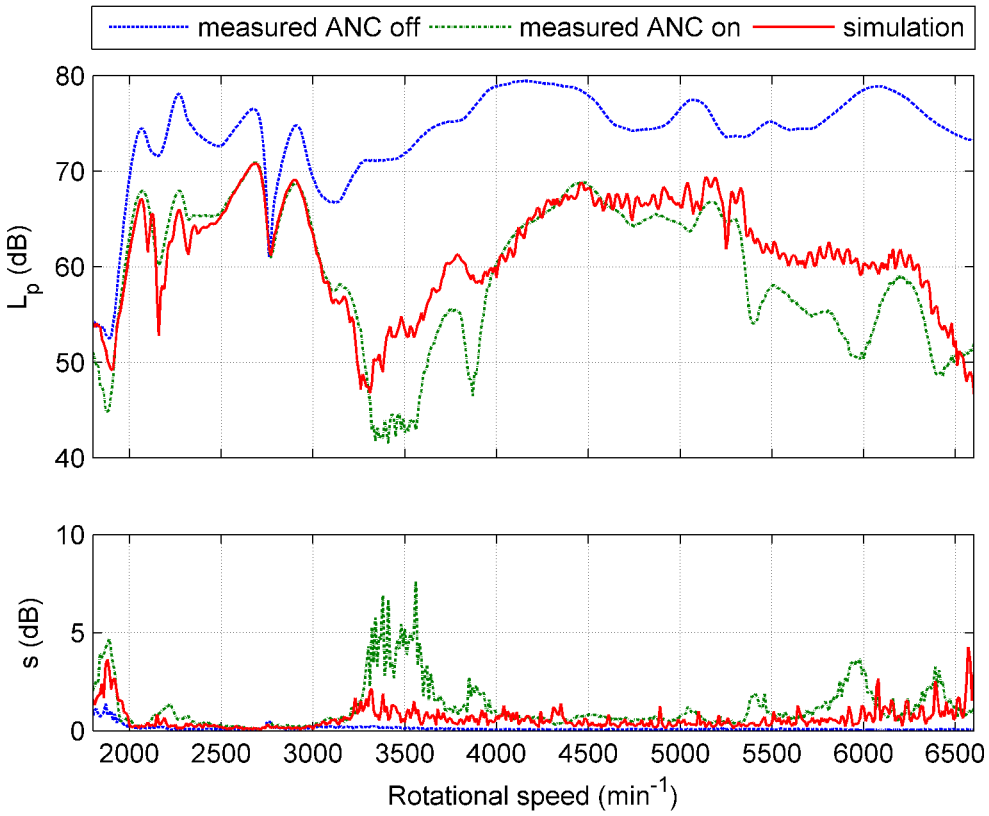

Figure 24. Averages and standard deviations of sound pressure levels of the second order as a function of rotational speed in the virtual sensor (Ch. 2) location.

The results are presented from Figure 24 to Figure 26 and in Appendix A. The averages and the standard deviations are calculated from eleven measurements with ANC on, from thirteen measurements with ANC off, and from eight simulation runs. Five of the simulation runs were discarded because the tachometric signal of the input recordings was corrupted and the measurement software was not able to detect it correctly.

The effect of background noise and round-off distortion in AD-DA conversions can be explicitly seen in Figure 24. In the measurement with ANC switched on, the standard deviation around a rotational speed of 3500 min^{-1} increases from one to five decibels. The corresponding sound pressure levels are just over 40 dB, so the random component of noise is significant in those levels and the adapting process becomes more random. In the simulation, like in Figure 24, the sound pressure level ripples a bit, but in the measurements such an effect is not present. An obvious reason for the difference was not found.

Overall, the correspondence between the measurements and the simulations is better than in the first measurement. In addition, the standard deviations of the simulations match those of the measurements more nicely. The standard deviations in this case support the explanation given in Section 5.3, where in the simulations the standard deviations at the error sensor location were higher than in the measurements. The hardest places for correct simulations seem to be in the error sensor, virtual or physical, locations, where sound pressures usually are the lowest. At low-level signals, the background noise has a greater effect. In the worst case, the differences in the results were 10 decibels, but all in all the correspondence between the measurements and the simulations is good.

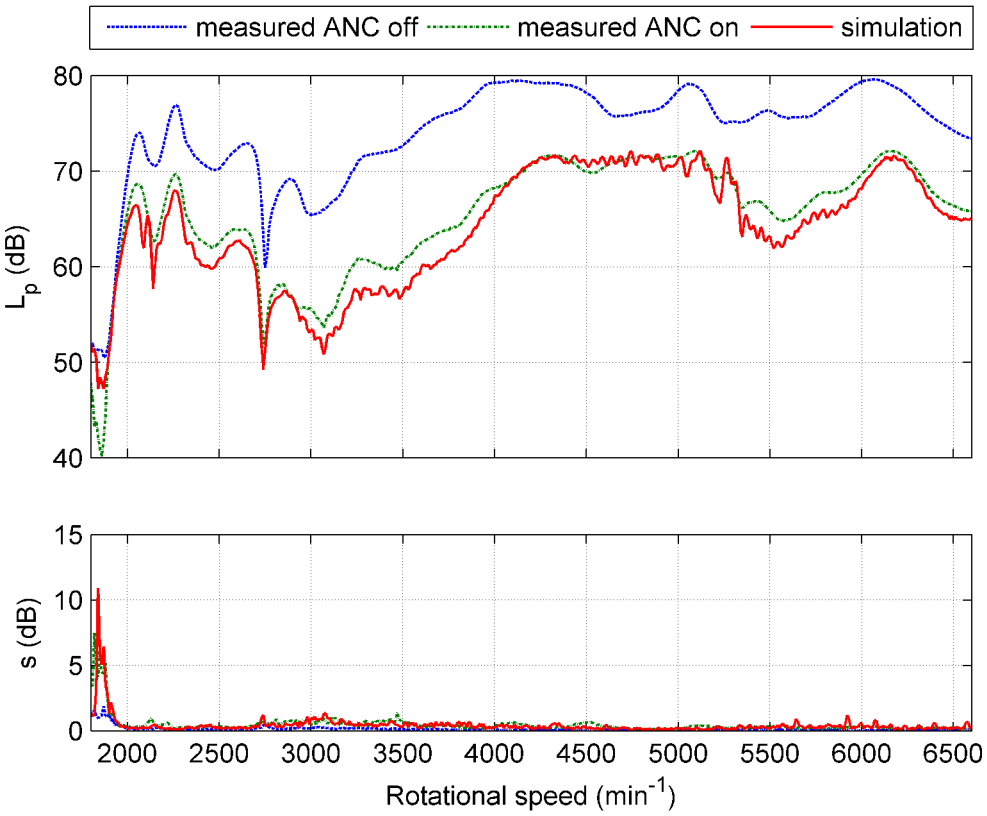

Figure 25. Averages and standard deviations of sound pressure levels minute of the second order as a function of rotational speed at the physical sensor (Ch. 1) location.

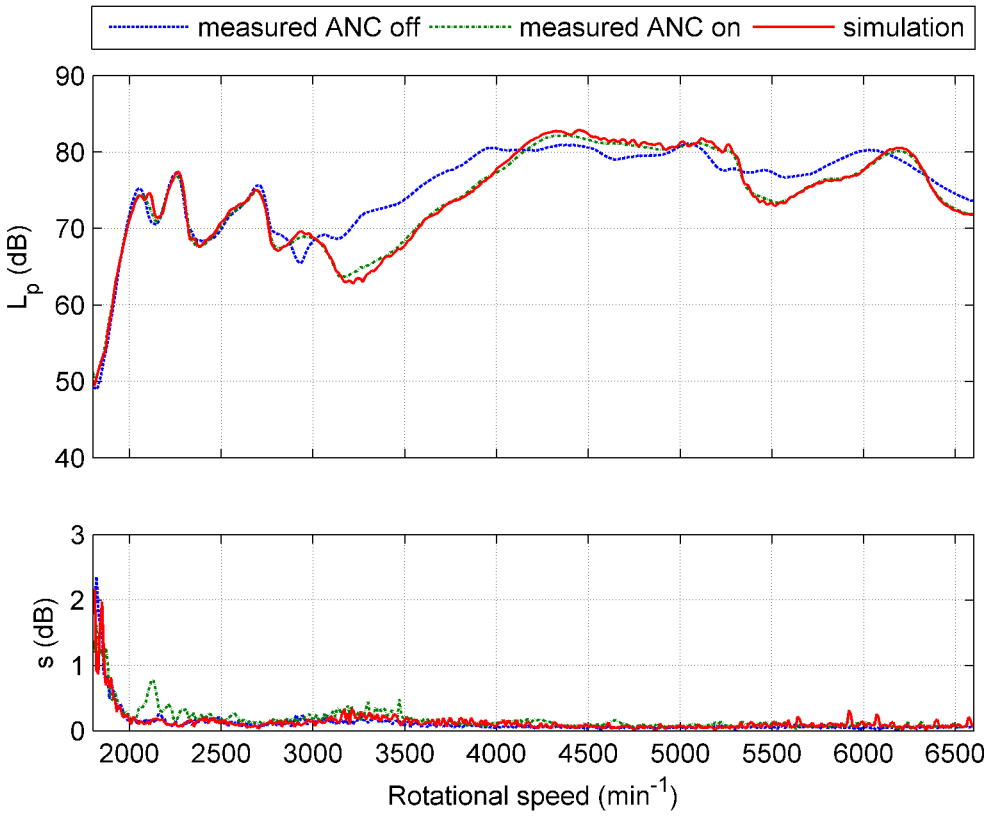

Figure 26. Averages and standard deviations of sound pressure levels of the second order as a function of rotational speed in the Ch. 3 location.

6 Conclusions and Future Work

A functional simulation model is a promising tool for developing practical active noise control systems. For example, through simulations the locations of transducers, the control algorithm variations and sound pressures at the ears of an observer can be tested without actual measurements. The major benefit of simulations is the repeatability of the simulation. Sometimes it is not evident what measurement results present unless you have the opportunity to repeat measurements accurately and change only one parameter between the measurements.

In this thesis, a simulation model of an active noise control system was developed and validated with measurements. In the simulations and the measurements the noise was periodical but its frequency content changed constantly over time. The validity of the simulation model was tested in three locations of an acoustic field. One of the locations was the error sensor of the control system and two others were randomly selected locations. The interest in the sound pressure in locations away from the error sensors was connected to the fact that in practical systems the error sensors are placed away from the ears.

The results presented here imply that the developed simulation model is capable of reproducing phenomena taking place outside the control system with a rather good accuracy. On the other hand, the simulation model presented here is not capable of reproducing phenomena taking place inside the control system because it was simulated with ideal blocks in a Simulink environment. For example, the computational limitations of the DSP card were not taken into account. Overall, the correspondence between the measurements and the simulations was good and better than was expected. For a generalization of the conclusions, simulations and measurements with a more complex primary noise and environment are needed.

In the future, more realistic simulation models can be made if, for example, the control system is implemented more non-ideally in the simulation model. With practical systems, it is more important to be able to reproduce fault conditions accurately instead of properly functioning system. For example, it might be beneficial to add noise and non-linear components inside the control system model. In addition, splitting the secondary path to the smaller elements would be useful. For example, in energy density sensing complex microphone arrays are used, so one would need more detailed models for the error sensors. Another question completely is when the complex control system models can be put into a model that simulate the whole sound field

and use the results when developing ANC systems. There are already some programs that should be capable of simulating such models, but nothing about the topic has been published yet.

Bibliography

[Bou91] **Boucher C.C., Elliot S.J.,** and **Nelson P.A.** "Effect of errors in the plant model on the performance of algorithms for adaptive feedforward control," *IEE Proceedings-F*, vol. 138, no. 4, pp. 313-319, August 1991.

[Bra05] **Brandt A., Lagö T., Ahlin K.,** and **Tuma J.** "Main Principles and Limitations of Current Order Tracking Methods," *Sound and Vibration*, pp. 19-22, March 2005.

[Cro97] **Crocker M.J.** "Noise Control" in **Crocker, M.J.** (editor) *Encyclopedia of acoustics Volume II*. New York, John Wiley & Sons, Inc. 1997.

[dBF04] *Order Analysis techniques used in dBRTA – dBFA software suite*, Limonest Cedex, 01dB-METRAVIB, 2004.

[Ell01] **Elliot S.** *Signal Processing for Active Control.* London, Academic Press, 2001.

[Ell88] **Elliot S.J., Joseph P., Bullmore A.J.** and **Nelson P.A.** "Active cancellation at a point in a pure tone diffuse sound field," in *Journal of Sound and Vibration*, vol. 120, no. 1, pp. 183-189, 1988.

[Ell92] **Elliot S.J.** and **Antonie A.** "A Virtual Microphone Arrangement for Local Active Sound Control," in *Proceedings of 1st International Conference on Motion and Vibration Control*, Yokohama, pp. 1027-1031, 1992.

[Fah85] **Fahy F**. *Sound And Structural Vibration: Radiation, Transmission and Response,* London, Academic Press Inc. 1985.

[Han01] **Hansen C.H.** *Understanding Active Noise Cancellation*. London, Spon Press, 2001.

[Han97] **Hansen C.H.** and **Snyder S.D.** *Active Control Of Noise and Vibration.* London, E & FN Spon, 1997

[Kar00] **Karjalainen M.** *Kommunikaatioakustiikka,* Espoo, Helsinki University of Technology, Laboratory of Acoustics and Audio Signal Processing, 2000.

[Koi07] **Koivo H**. *Tietokonesimulointi,* Espoo, Helsinki University of Technology, Control Engineering Laboratory, 2007.

[Kuo96] **Kuo S.M.** and **Morgan D.R.** *Active Noise Control Systems Algorithms and DSP Implementations*. New York, John Wiley & Sons, Inc. 1996.

[Mat07] *MATLAB R2007B help,* The MathWorks, Inc., 2007.

[Mis99] **Miskiewicz A.** and **Letowski T.** "Psychoacoustics in the Automotive Industry," *Acta Acustica united with Acustica,* vol. 85, no. 5, pp. 646-649, September 1999.

[Mor68] **Morse P.M.** and **Ingard K.U.** *Theoretical Acoustics*, New York, McGraw-Hill, Inc, 1968.

[Nel92] **Nelson P.A.** and **Elliot S.J.** *Active Control of Sound,* London, Academic Press Inc. 1992.

[Pea02] **Pearsall J.** (editor), *The Concise Oxford English Dictionary, 10th edition (revised),* Oxford, Oxford University Press, 2002.

[Pop97] **Popovich S.R.**, "Active acoustic control in remote regions", US Patent No. 5,701,350, 1997.

[Obe04] **Oberkampf W.L., Trucano T.G., Hirsch C.** "Verification, validation, and predictive capability in computational engineering and physics," in *Applied Mechanics Reviews,* vol. 57, no. 5, pp. 345-384, September 2004.

[Ree06] **Rees L.E.** and **Elliot S.J.** "Adaptive algorithms for Active Sound-Profiling," in *IEEE Transactions on Audio, Speech, and Language Processing,* vol. 14, no. 2, pp. 711-719, March 2006.

[Ros02] **Rossing T.D., Moore F.R.,** and **Wheeler P.A.** *The Science of Sound, 3rd edition,* San Francisco, Addison Wesley, 2002.

[Rou99] **Roure A.** and **Albarrazin A.** "The remote microphone technique for active noise control," in *Proceedings of Active '99,* Florida, pp. 1233–1244, 1999.

[Sch79] **Schlesinger S.** "Terminology for model credibility," in *Simulation,* vol. 32, no. 3, pp. 103-103, 1979.

[Spe03] *TMS320C6713 DSK Technical reference.* Stafford, Spectrum Digital Inc, 2003. Available also online at http://c6000.spectrumdigital.com/dsk6713/V2/docs/dsk6713_TechRef.pdf Checked February 1st 2008.

[Sta02] **Stan G., Emprechts J., Archambeau D.** "Comparison of different impulse response measurement techniques," in *J. Audio Eng. Soc.*, vol. 50, no. 4, April 2002.

[Tan95] **Tanttari J.,** and **Saarinen K.** *Työkoneiden melun vähentäminen – perusteet,* Tampere, Metalliteollisuuden Keskusliitto, 1995.

[Tex04] *TLV320AIC23B Stereo Audio CODEC 8- to 96-kHz, With Integrated Headphone Amplifier Data Manual*, Dallas, Texas Instruments Inc., 2004. Available also online at http://focus.ti.com/lit/ds/symlink/tlv320aic23b.pdf Checked February 1st 2008.

[Wel67] **Welch P.D.** "The Use of Fast Fourier Transform for the Estimation of Power Spectra: A Method Based on Time Averaging Over Short, Modified Periodograms," in *IEEE Trans. Audio Electroacoustics,* vol. AU-15, no. 2, pp.70-73, June 1967.

Appendix A

Measurement Data

The rest of the measurement data that was presented in Chapter 5 is presented in here.

Measurement with Control System Using Active Noise Profiling

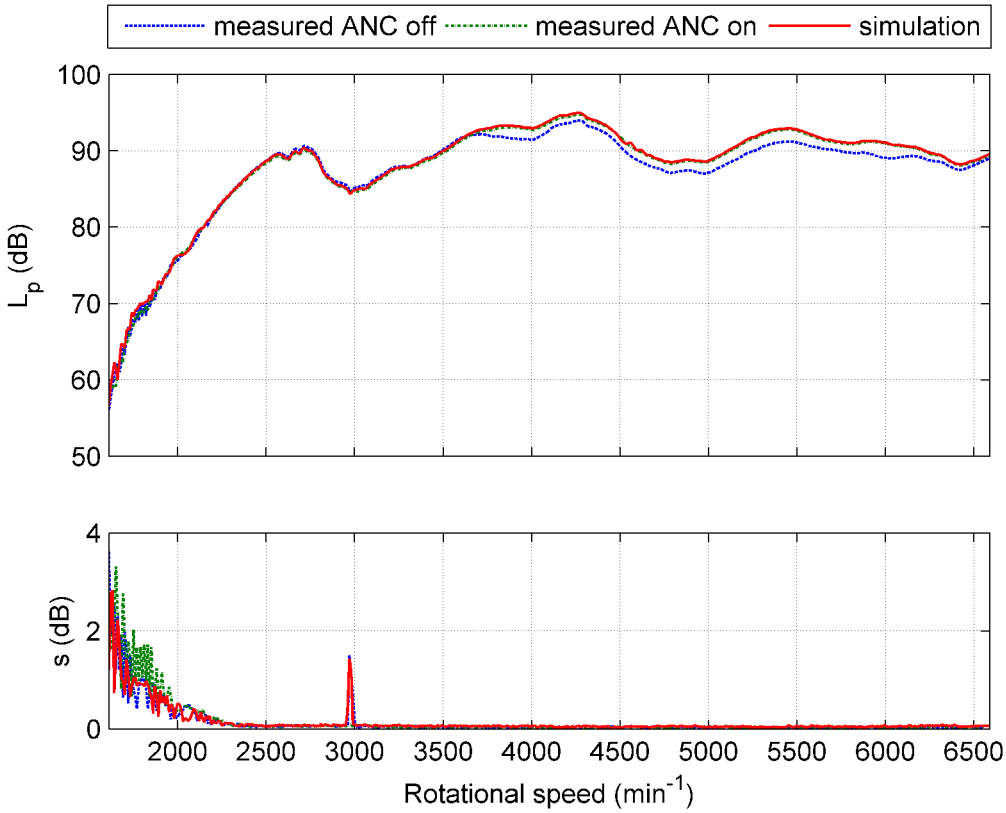

Figure A 1. Averages and standard deviations of sound pressure levels of the second order as a function of rotational speed in the Ch. 2 location.

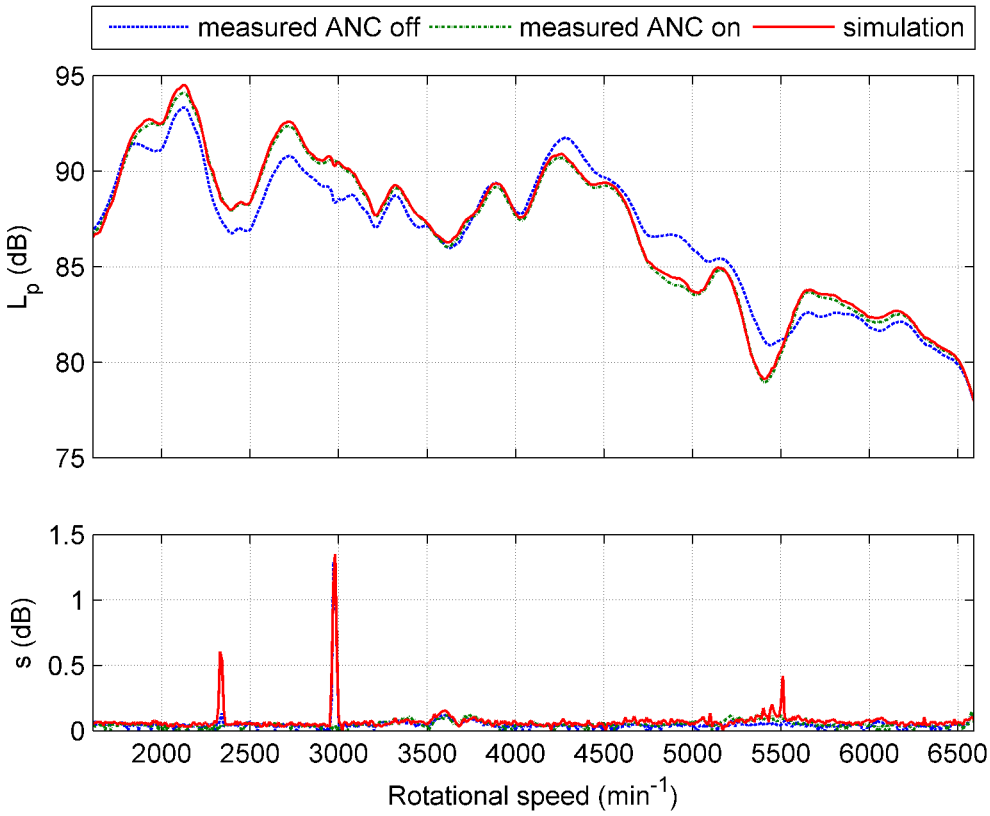

Figure A 2. Averages and standard deviations of sound pressure levels of the fourth order as a function of rotational speed in the Ch. 2 location.

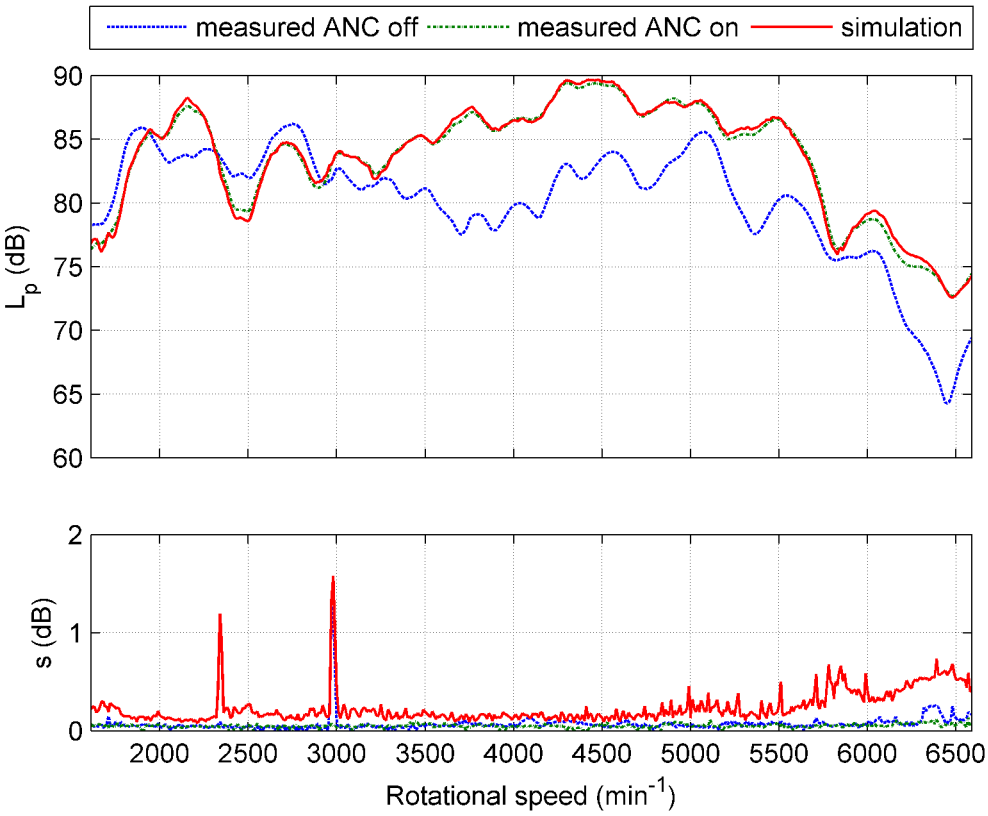

Figure A 3. Averages and standard deviations of sound pressure levels of the fourth order as a function of rotational speed in the Ch. 3 location.

Measurement with Control System Using Virtual Microphone

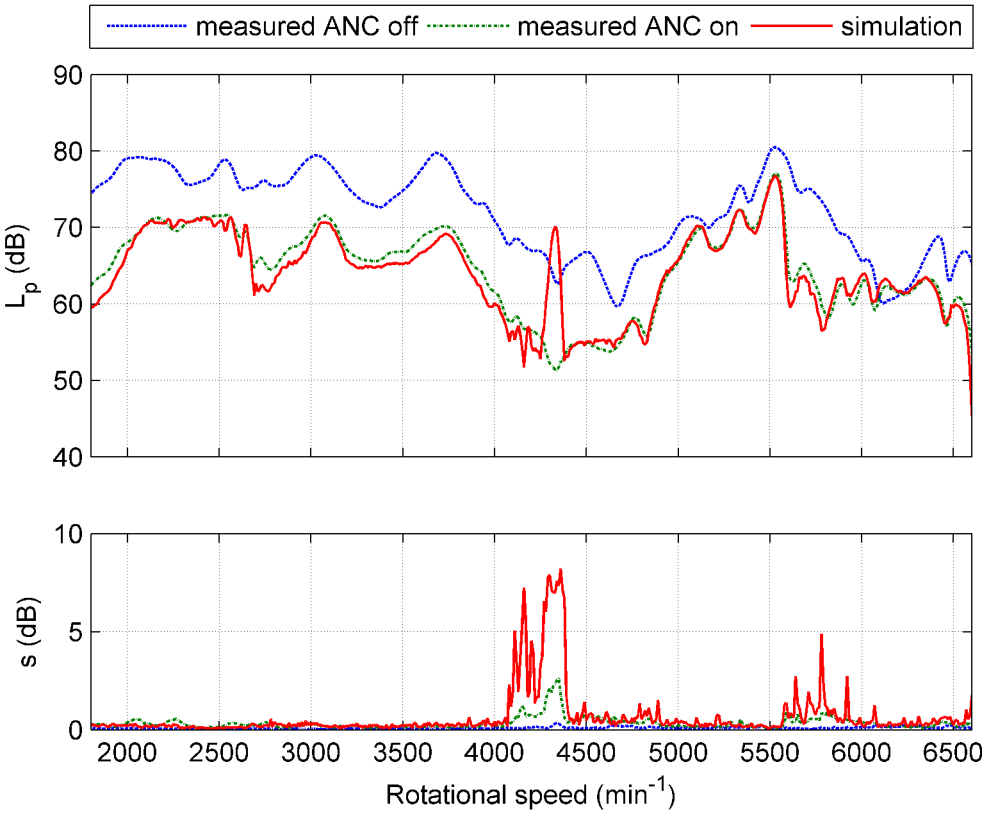

Figure A 4. Averages and standard deviations of sound pressure levels of the fourth order as a function of rotational speed in the physical sensor (Ch. 1) location. In the simulations, the peak around 4300 min^{-1} is due to the instability of the adaptation process.

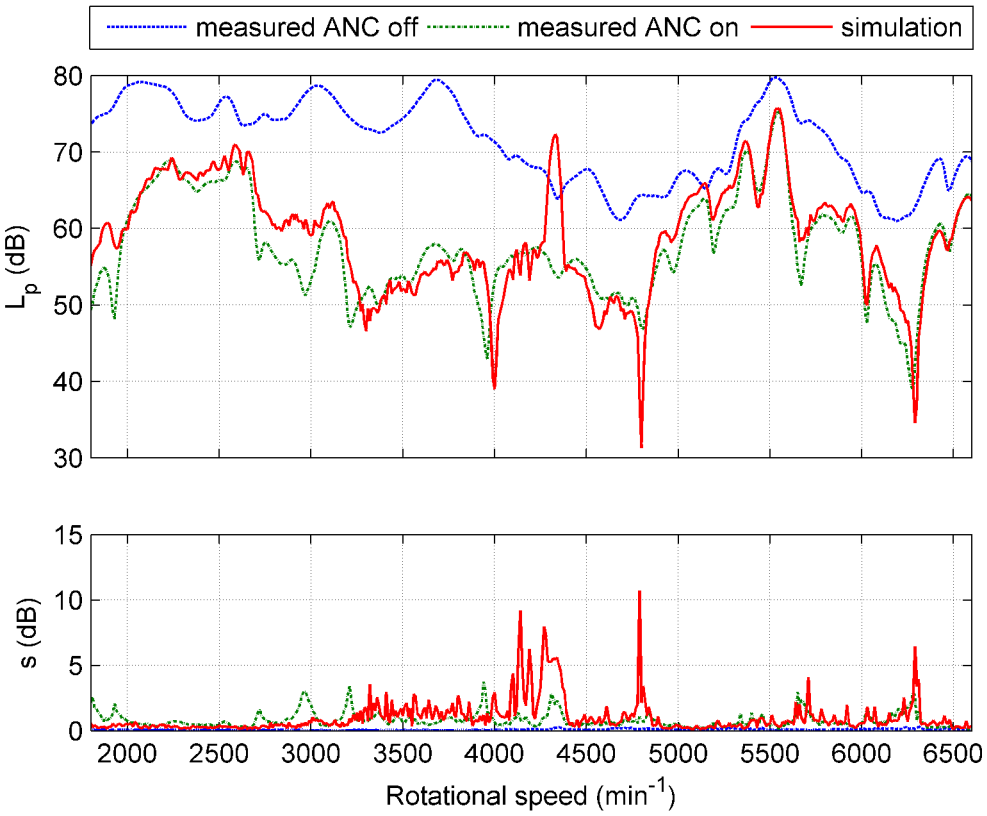

Figure A 5. Averages and standard deviations of sound pressure levels of the fourth order as a function of rotational speed in the virtual sensor (Ch. 2) location. In the simulations, the peak around 4300 min^{-1} is due to the instability of the adaptation process.

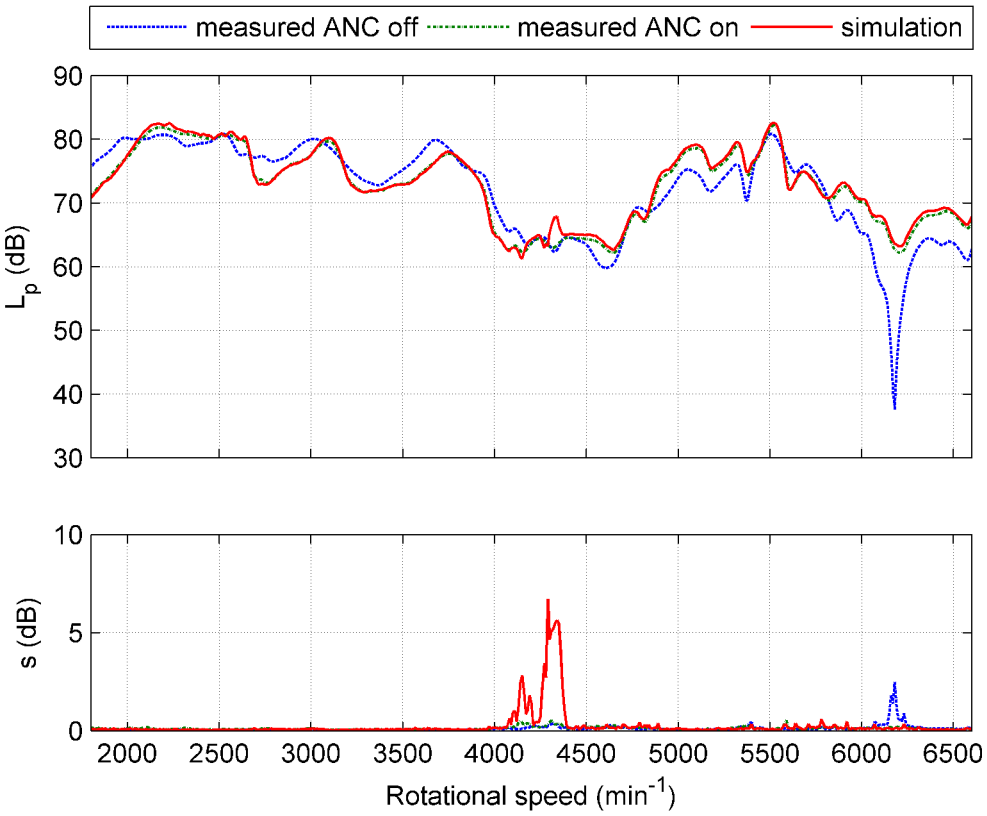

Figure A 6. Averages and standard deviations of sound pressure levels of the fourth order as a function of rotational speed in the Ch. 3 location.